U.S. Department of Energy, Energy Efficiency & Renewable Energy

Final Technical Report DE -EE0006284.0000

Multidisciplinary Design of an Innovative Natural Draft, Forced Diffusion Cookstove for Woody and Herbaceous Biomass Fuels in East Africa

Project Period: 09/15/2013-09/14/2017

PI: Jonathan D. Posner
Professor of Mechanical Engineering and Chemical Engineering
University of Washington
jposner@uw.edu, 206.543.9834

Lynette Arias
Director, Office of Sponsored Programs
University of Washington
Office of Sponsored Programs
4333 Brooklyn Ave NE Box 359472
Seattle, WA 98195-9472
206-543-4043 | osp@u.washington.edu

September 12, 2018

DUNS: 605799469
University of Washington
Stevens Way, Box 352600
Seattle, WA 98195

This material is based upon work supported by the Department of Energy under Award Number DE - EE0006284.0000

1. Objectives

The goal of the project was to develop a commercially viable, natural draft cookstove that exceeds ISO tier 4 criteria while meeting the needs of rural and urban cooks in East Africa. The cookstove should be market ready that meets the manufacturing cost and usability expectations of the final users, including durability, safety, comfort, aspirational value and compatibility with local fuels, foods, and customs. The cleaner burning cookstove product was designed to replace open fires and inefficient stoves so that it can enhance indoor air quality, personal health, livelihoods, and the environment. The stove was developed using integrated and multidisciplinary design approach that included field based user research and focus groups, empirically verified computational fluid dynamics and heat transfer modeling, lab and field based emission and efficiency measurements, design for manufacturability, as well as in-home user product evaluations.

2. Approach

The project started with field-based user research the goal of determining what characteristics and features of improved cookstoves are preferred by potential cookstove users. To gather this information, a series of IRB approved focus group discussions (FGDs) and home placements were made in five different geographic areas in central and western Kenya. Five project prototype cookstoves together with four commercially available cookstoves were used in the study. A total of 213 participants took part in the FGDs. These participants were selected for the study based on their age (18 – 58), the primary fuel used for cooking (firewood), and their socio-economic status (monthly expenditures of 1001 to 10,000 Ksh). The cooks came from households of two to eight people. We also recorded information on the size, type, and quality of the wood they used to cook as well as the number and types of pots they used. The typical wood and pots used is important for the stove design because it impact performance.

Throughout the project we use computational fluid dynamics (CFD) and heat transfer modeling to aid in the design of efficient and clean burning stoves. The CFD models include combustion, heat transfer, and fluid flow and a variety of stove geometries, model dimensionalities, turbulence models, combustion chemistries that depend on the question to be answered. One goal of this work was to develop high fidelity models that can be used to design stove components that result in an overall clean and efficient stove approaches. In addition, the CFD models could be used to elucidate the flow and heat transfer phenomena in the stove and inform generalized stove design principals. These models provided detailed information of the fluid flow, combustion chemistry, stove component temperatures, and stove efficiency.

One of the primary objectives was iterative design, stove fabrication, and lab based stove testing. The stove designs are informed from the field-based user research and the computational modeling. Dozens of stoves were designed, fabricated, and tested in the lab using International Organization for Standardization (ISO) Water Boiling Test (WBT) as well as several other newly developed testing protocols. The experiments informed the CFD models and were used to provide metrics for the stove performance relative to the target stove performance goals. A novel, real-time particulate matter emissions system was developed that enabled rapid evaluation of stoves over a wide range of stove operation conditions such as firepower. Individual stove components and integrated stoves where evaluated relative to performance targets.

Highly performing stoves that were expected to meet the technical performance targets as well as the users needs were evaluated in the homes of rural East Africans. Fifteen homes were evaluated with ten improved cookstoves and five traditional three-stone fires. Uncontrolled cooking tests were performed while emissions were measured. This information was used to evaluate the improvement of efficiency and emissions relative to traditional stoves as well as provide feedback to the design process.

The stove design that met all the performance targets and the user's needs underwent a design for manufacturing process with the goals of reducing parts, cost, and assembly time as well as reducing stove cost. The modified stove underwent accelerated durability testing in East Africa in the goal of simulating three years of use. Failure mechanisms were evaluated and several stove components were modified or eliminated. This stove was Tier 3 performance in all but two categories.

The ultimate goal of the project was to deliver a market ready stove design that could be manufactured at scale and that met the usability expectations of the final users, including durability, safety, price, comfort, aspirational value and compatibility with local fuels, foods, and customs. Our proposed goal was to have a design that

manufacture ready; however, near the end of this project Burn Manufacturing Company (BMC), the sister company of the project's nonprofit project partner Burn Design Labs, obtained external investment from Unilever and Acumen to bring cleaner, more affordable cook stoves to smallholder farmers and plantation workers in East Africa. BMC adopted the stove developed in this project and used the Unilever and Acumen funds to purchase tooling and get a new manufacturing line up and running to manufactur the stove. The commercial product stove is called Kuniokoa which is Swahili for "wood saver."

3. Results

In this section we provide a brief overview of the results from each activity.

3.1 Field User Research

The purpose of this study was to determine the cuisine, fuels, tools, and methods that potential cookstove users employ. In addition, we were also interested in the characteristics and features of improved cookstoves that are preferred or acceptable to users. To gather this information, we conducted a series of focus group discussions (FGDs) and home placements in five different geographic areas in central and western Kenya. Five UW prototype cookstoves and four commercially available cookstoves were used in the study. A total of 213 participants who use wood for fuel were selected for the study based on their age (18 – 58) and their socio-economic status monthly expenditures of 1001 to 10,000 Ksh. Nearly half of the cooks were using some form of improved cookstove in their homes at the time of this study. The balance other half of the participants were using 3-stone fires for cooking at home. The majority of the cooks gathered their wood while 35% of the cooks purchased wood at an average price of 370 ksh/week.

Study Design

A longitudinal design was used in the study 213 cooks that participated in the first phase of user research in five geographic locations. Forty six respondents were recruited in each of the five research sites; but not all participated in focus group discussions (FGDs). Cooks were drawn from the C1, C2 and D market segments according to a segmentation study that was conducted in Kenya, households could be categorized based on the expenditure of households. Monthly expenditure was used as a basis for categorization as follows:

Less than Ksh 1000	E
1001 to 3000	D
3001 to 6000	C2
6001 to 10,000	C1
Above 10,000	AB

Each target market segment was expected to comprise 12 cooks; 36 in total. A group of 10 women leaders drawn from the target market segments were recruited, in each of the five study sites. These key opinion leaders were drawn from women groups, church, political leaders and community health workers. A total of 213 cooks who participated in the study responded to a brief semi-structured questionnaire, to collect data on fuel types used in different geographic sites, sources of fuel and cooking practices, prior to participation in focus group discussions. Thereafter, some cooks were selected to participate in the home placement activity. Each cook was advised to use the prototype cookstoves for 24 hours followed by data collection the following day using an in-depth interview guide.

The first phase of user research was conducted in five sub-counties: Gatanga, Meru, Kericho, Narok and Vihiga. Sampling was used to select sub-counties of study based on fuel types used in various regions. A convenient sample size of 213 was used rather than calculate a sample size based on population in study areas since our focus was on qualitative aspects of the rocket stoves prototypes. Nine prototype and commercially available stoves were used in the study.

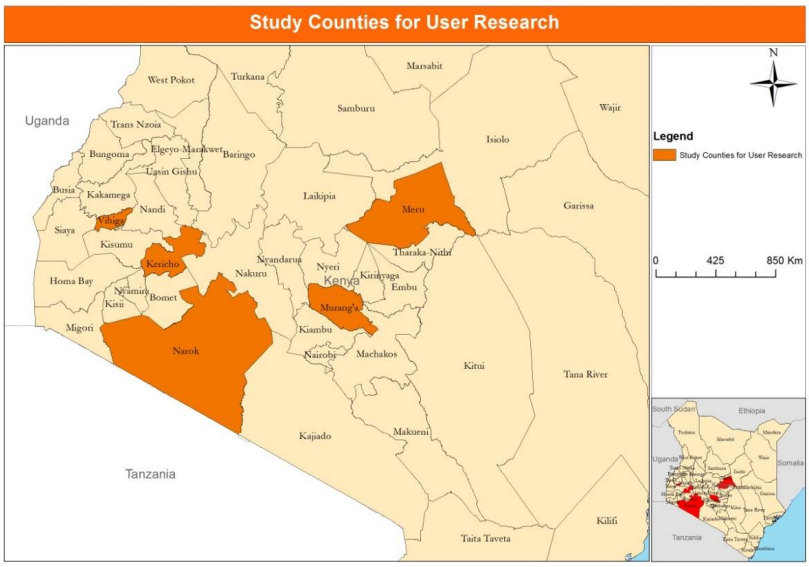

Figure 1. Map of user research locations in East Africa.

The user research was lead by Paul Means and Dr. Constance Ambosa with the assistance of Pauline Oudo , Siku Mathii , Janerose Kweyu , Hellen Mudia and Beula Achieng. Mr. Means, the director of Burn Design Labs was the US lead and Dr. Ambosa, a PhD trained sociologist who speaks Swahili, coordinated the efforts in East Africa. She recruited several other facilitators as shown in the image below.

Figure 2. User research team from left to right: Pauline Oudo , Siku Mathii , Janerose Kweyu , Hellen Mudia (standing) , Constance Ambosa (standing),and Beula Achieng.

Ecozoom

Baseline stove with extended deck

Baseline stove with door

M-5000

Tall Baseline stove

Econofire TM

Baseline w/ extended deck & swing door

Short Baseline Stove

Jiko Chap Chap

Figure 3. Cookstoves used in User Research in Narok and Vihiga Counties

Table 1: Dimensions of stoves used in the focus group studies.

Stove Type	Weight	Height	Cone Deck Diameter
D-M 5000	3962g	27.5 cm	25cm
C-Ecozoom-	7614g	25cm	28cm
Baseline-	3888g	36cm	28cm
Baseline with swing door	3878g	36cm	28cm
Baseline with extended deck-	3860g	36cm	34cm
Short baseline-	3332g	30cm	28cm
Econofire TM	2758g	24cm	38cm
Baseline w/ an Extended Deck	4484g	36cm	34cm
Jiko Chap Chap*	6500g	51cm	33cm

**Jiko Chap Chap was used at Kericho Finlay research site only. Attempts to obtain another sample for use in Narok & Vihiga were unsuccessful. A modified baseline stove with an extended deck & swing gate was first introduced at the Kericho site based on findings from Gatanga and Meru.*

Figure 4. Pilot study focus group. The faces have been blurred to retain the participants privacy.

Socio-Economic Characteristics of Respondents

Many cooks [86, 40%) belonged to the C1 socio-economic group with monthly income between Ksh 6,001 and Ksh 10,000 [USD 71 and 118] (Figure 2). Next was C2 socio-economic group [74, 35%] and D [53, 25%] with monthly income between Ksh 3,001 and Ksh 6000 [USD 35 and 70.5] and between Ksh 1001 and Ksh 3000, [USD 12 and USD 35], respectively. Most cooks in Narok County belonged to the high socio-economic group [C1=25, 57%] compared with Vihiga County where many cooks [18, 42%] belonged to D socio-economic group. Overall, cooks in Kericho County had the highest monthly income with an average of Ksh 10,000 while Vihiga had the lowest monthly income with an average of Ksh 3,100.

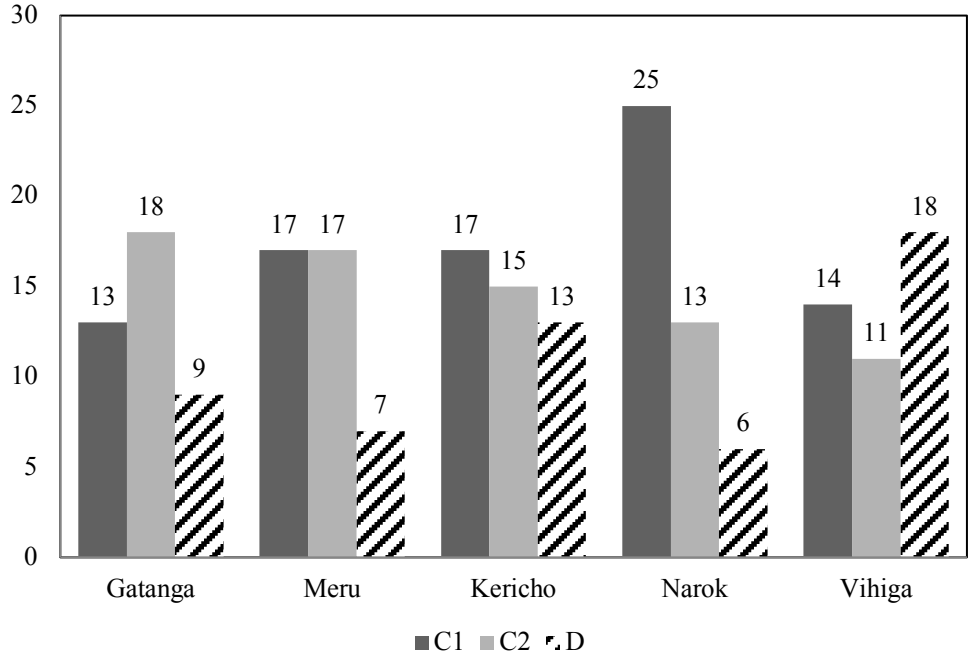

Figure 5. Socio economic class of cooks who participated in upfront user research focus groups.

The age of cooks ranged between 18 years and 58 years. An equal number of cooks belonged to the 25-34 and 35-44 year old brackets. Cooks in Kericho County were mostly young because tea picking and factory work are labor intensive. Cooks in Gatanga and Vihiga counties were older. Age has a bearing on adoption of cookstoves. Younger cooks are likely to generate more cash for buying improved stoves compared with the elderly who may resist change altogether in preference for traditional three stone fire.

Cooks in Kericho and Narok Counties had fewer people in their households [between 3 and 4] compared with Meru and Vihiga Counties where some households comprised 12 members (Figure 4). Polygamy is practiced in Narok County and families are usually large. Many cooks that participated in user research still had small families that comprised between 3 and 4 people. However, there were some families with 8 members and above in the same county. The size of HHs influences preference or some features of cookstoves.

All 213 cooks used firewood as their main source of fuel; especially in Kericho and Vihiga Counties with limited use of other fuel types (Figure 5). Most cooks in Narok County [35, 80%) also used charcoal to cook. because the stable food of the Maasai is roast meat. Charcoal, is therefore, required to facilitate grilling and roasting of beef & mutton.

Apart from a few cooks, the majority in Narok and Kericho Counties did not purchase firewood unlike those in Vihiga County (Figure 6). The source of firewood in Narok County was the forest and neighborhood while at Kericho, tea bushes were mainly used as sources of firewood. There was also limited access to firewood from woodlands that are planted and protected by management of Finlay Tea Factory.

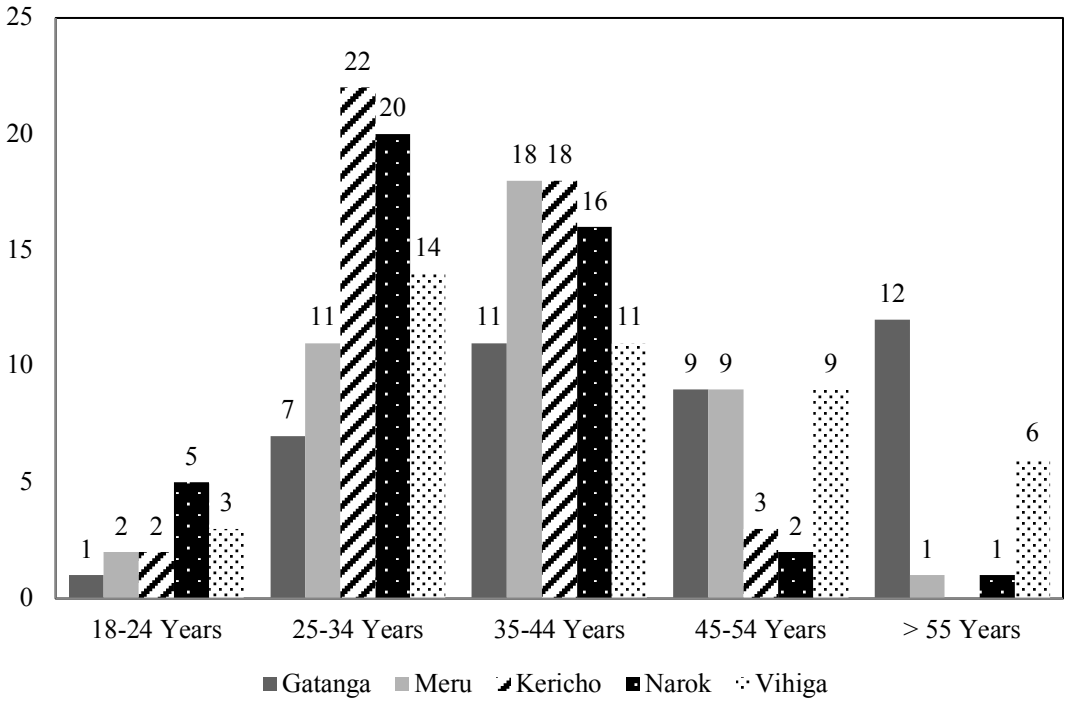

Figure 6. Histogram showing age of cooks who participated in the study by region

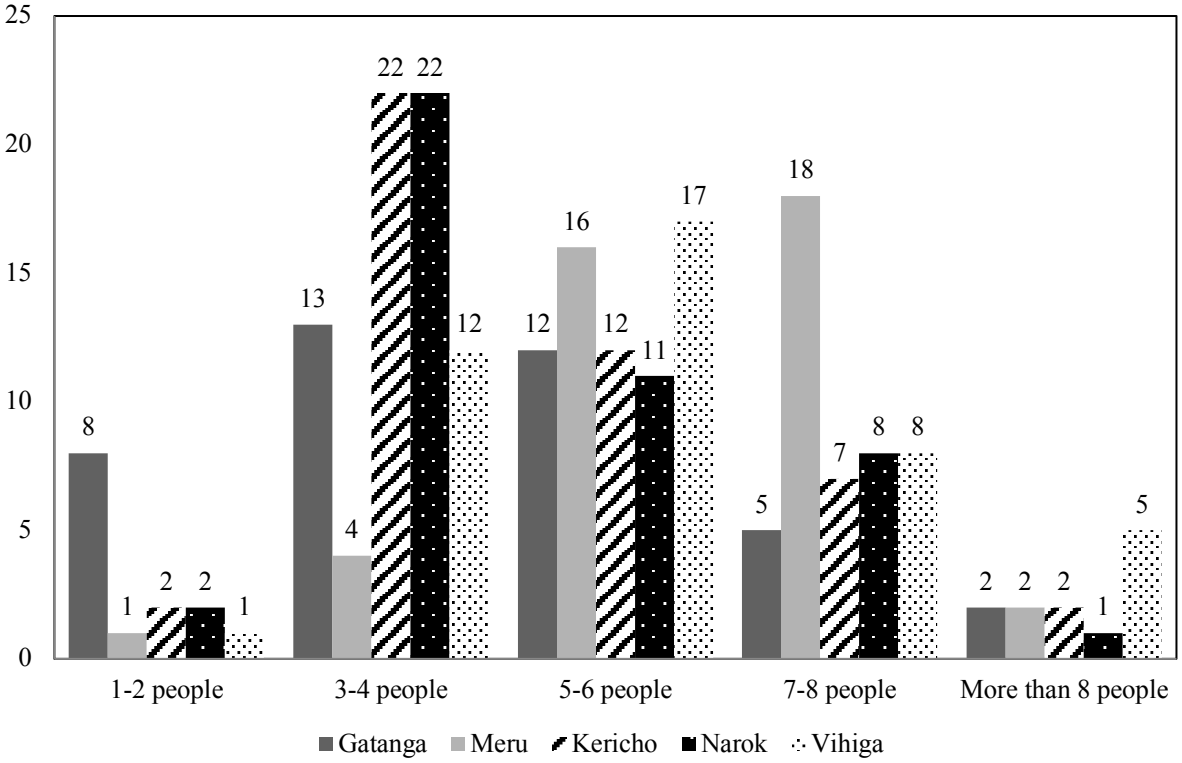

Figure 7. Size of households of focus group participants by region.

The cost of firewood was cheaper at Kericho (it ranged between 1-200 Ksh per week] with an average of 120 Ksh compared with Vihiga County where the cost of firewood was highest with a mode of 500 Ksh. Some cooks spent over 500 Ksh on firewood per week in Vihiga County because it is among the most densely populated areas in Kenya. Most vegetation cover has been cleared to create room for settlement and agricultural activities. Few cooks derive firewood from their own farms. The majority purchase it from markets or farmers in their neighborhoods. The average cost paid for firewood, by those who buy wood, was approximately 370 ksh/week.

All cooks at Kericho used brick rocket stoves because these stoves were installed in all houses in the tea estate. Whereas cooks in Meru and Gatanga used jiko Kisasa. Participants in Vihiga used three stone fires and portable clay stoves. Cooks at Narok used three stone fires.

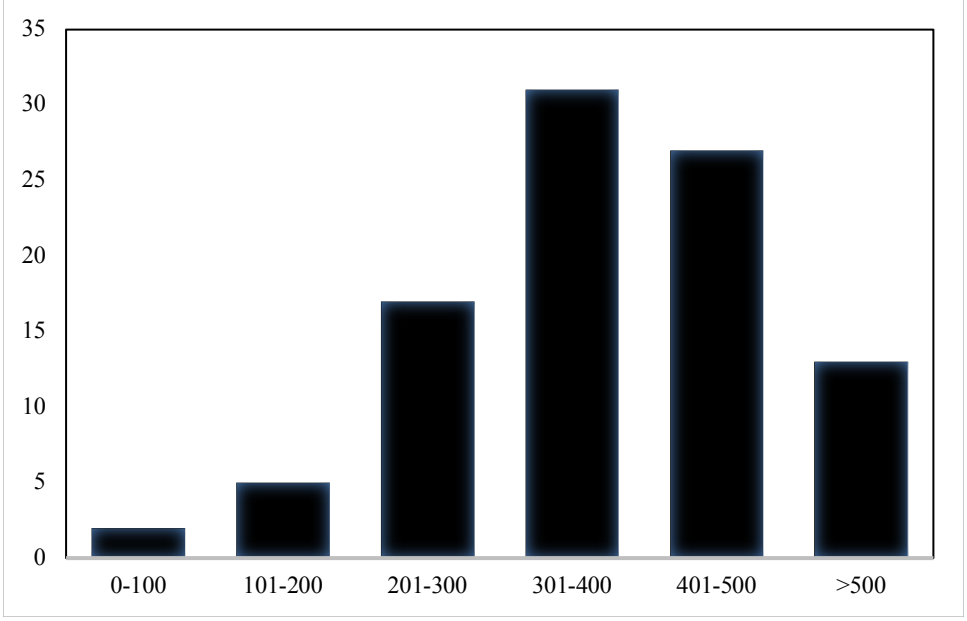

Figure 8. Histogram of cost of wood per week in Ksh.

Figure 9. Sample traditional cooking areas in Kericho and Vihiga

Preferences of Users

We obtained users impressions before and after the use of the cookstoves and noted how perceptions of stoves and stove features changed based on their experience. Before running the stoves, users generally preferred heavier stoves, such as the Ecozoom Dura Stove, because of the impression that the stove was durable, would support large heavy pots of food, and that the stove would retain heat. Some cooks [32/215, 15%] preferred a UW prototype stove with a swing gate because they believed it could cook fast, the swing gate could retain heat and the stove could save on fuel. Other reasons given for pre-cooking preferences included strong handles, heavy pot supports, use of ceramic, an ash tray, a swing door, and the color & attractiveness of the stove.

After cooking with the stoves, the perceptions changed. The most preferred stoves in a descending order were the UW baseline prototype stove with a swing Gate [63/213, 30%], baseline stove with an extended deck [51/213, 24%], and baseline stove [35/213,16%]. Some cooks switched their preferences of shorter stoves that appeared more attractive to taller ones that cooked fast during post-cooking phase. Whereas 66 cooks had preferred the Ecozoom Dura stove in the pre-cooking phase, only 24 cooks preferred it in the post-cooking phase. After the cooks had had an opportunity to cook a meal on the stoves, their preferences for stoves were based primarily on good fuel efficiency, low particulate emissions, speed of cooking and ease of lighting. Other reasons included the height of the stove (suitable for tending the stove while seated), ability to support large pots, light weight (easy to carry), and attractive appearance.

The moderately sized 88 cm^2 feed chamber opening of the Burn stoves was preferred by over half of the participants. Other stoves, with both larger (91 cm^2) and smaller (70 cm^2) fuel feed chambers openings, split the remaining votes for preference. This infers that the feed chamber opening size of the Burn stoves is close to optimum. All cooks preferred an ash tray over no ash tray. In terms of an ash tray handle, cooks largely preferred an ash tray handle design that faced downwards so that it did not get hot while the stove was in use.

Over two- thirds of the cooks preferred the cast metal handles with rubber cover, of the type on the baseline stove. Nearly 80% of the cooks were willing to use a pot skirt but the rest of the cooks did not want to use a pot skirt at all. Surprisingly, those who were willing to use a pot skirt valued it more as a way to firmly hold the pot while cooking ugali, a stiff corn meal-based porridge that requires vigorous stirring, more than as a fuel saving addition to the stove. As for the design of the pot skirt, ¾ of the cooks preferred the design that allowed for easy removal of the pot from the skirt. Unfortunately, the handles on the pot skirts were too hot so some cooks used newspaper to insulate the handles. Also, Burn stoves appeared to accumulate more soot when pot skirts were used than when not used. It was difficult for cooks to associate such increased soot accumulation with improved efficiency

Over 80% of the cooks preferred a stove with an extended deck. Preference for an extended deck was 100% in those communities with large households, because and extended deck is thought to better accommodate large pots. Two thirds of the cooks preferred a swing gate (door) on the fuel feed chamber because they understood this feature to help conserve fuel. Those cooks who did not prefer a swing gate felt that it would hinder feeding fuel into the stove. Initially (pre-cooking) there was less acceptance of the swing gate because it made it more difficult to see the flame. After the cooking experience with the stove, the cooks were more comfortable to with a higher efficiency stove with a less visible flame. Although just over 60% of the participants preferred the type of pot supports on the Burn Design Lab Stoves, the reasons were not entirely clear. Pot supports like those on the Ecozoom Dura stove were preferred by about 1/3 of the participants who cited the thick/heavy material as a determining factor. Over 2/3 of the cooks preferred the solid sheet metal support rack for the sticks (fuel). The heavy wire rack used on the Ecozoom Dura was also well liked. A thin (3 mm) wire grate support rack introduced later in the study was perceived to be too weak.

Fuel Source Details

During the field studies, we collected data on the wood fuel moisture and size. This information is useful because it enables the designer to stove consistent with its operation by users. Specifically, the combustion chamber can be dimensioned according to the range wood used as well as lab based experiments can be conducted with fuel consistent with availability in the field. We measured the wood fuel moisture with a hand held conductivity moisture meter. Note that the fuel moisture histogram shows a bimodal distribution. A broad base of cooks complained about the fuel moisture being unacceptably high when it was above 20% by weight. The

cross section of the fuel sticks was approximately uniform along the length of the sticks. The fuel size was determined by measuring the cross section of the fuel at it widest and narrowest and by noting the general cross section shape, either rectangular, triangular, or circular (oval). We report the diameter as the hydraulic diameter that is calculated as four times the area divided by the perimeter. The average fuel size was 3.8 cm and the size ranged from 1 cm to over 10 cm.

Overall, these upfront user research studies gave the team bounds on acceptable features, the size and moisture of the fuel source, and general perceptions of what potential stove customers value and what they are willing to may be willing to pay for.

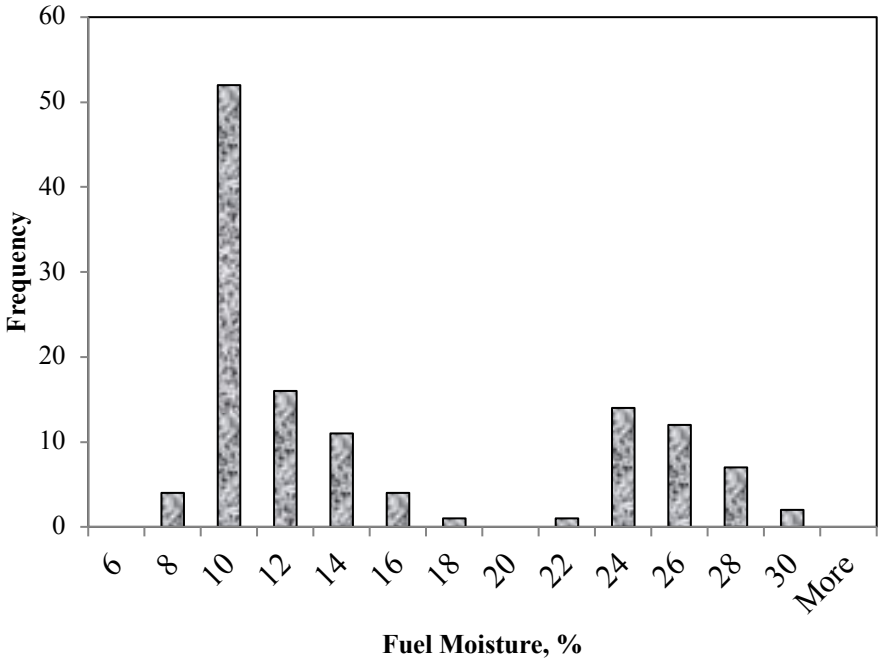

Figure 10. Moisture Distributions of fuel samples taken during focus group discussions in Narok, Kericho, and Vihiga.

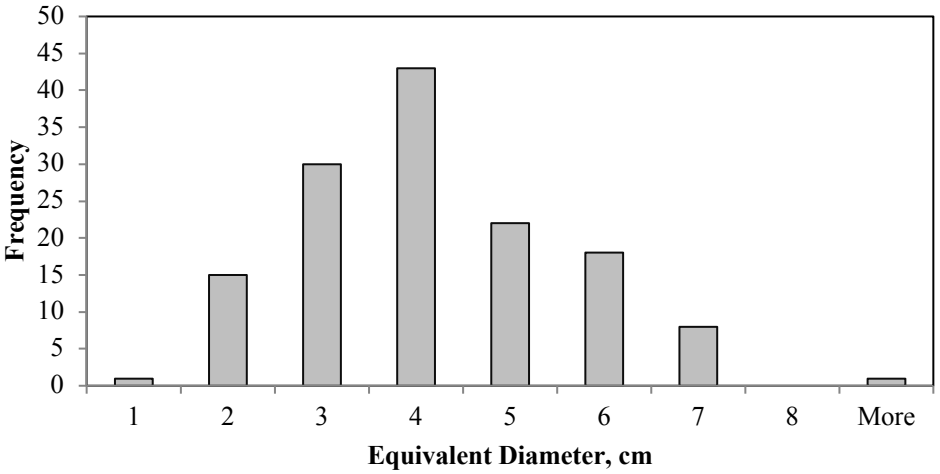

Figure 11. Size and distribution of fuel sticks used during focus group discussions in Narok, Kericho, and Vihiga.

3.2 Cookstove Modelling

Most stoves are designed using a purely iterative process, i.e., building a prototype, testing it, then refining stove parameters until an acceptable design is found. This Edisonian design process is resource intensive, time consuming, and often does not provide insight into the physics inside the cookstove, such as combustion, heat transfer and fluid flow. Computational modeling is an attractive complement to building and testing stoves, as it is more cost-effective and a large number of variations can be evaluated efficiently. Several combustion systems such as internal combustion engines, gas turbines and thermal power plants have achieved improved performance using numerical simulation. Numerical models also have the capability to provide details about physical processes inside the cookstove, the knowledge of which can be used by stove designers to design better performing natural draft cookstoves. The effect of geometric parameters on combustion and mixing can also be studied without undergoing the expensive and time-consuming process of building and testing cookstoves.

There are few reports of numerical simulations of cookstoves. In the last thirty years, five hundred journal articles have been published on cookstove development, but fewer than thirty have focused on modeling [1]. Early modeling work was conducted by Baldwin [2] who developed a steady-state heat transfer model to study the effect of the length and width of the channel between the cookpot and pot skirt on the heat transferred to the cookpot. The model predicted that a smaller channel gap and longer channel length increased the heat transfer to the pot, but this was not experimentally validated. The model used several unrealistic assumptions, and the author cautioned against its use as a predictive tool. Agenbroad et al. [3], [4] developed a Bernoulli equation based model with a constant loss coefficient to predict the flow rate through a rocket elbow without a pot, given the geometry of the elbow and the firepower. The model was validated with excess air and temperature measurements for a range of firepowers. The model results were sensitive to the loss coefficient, which was used as a model tuning parameter.

CFD based models of cookstoves have also been developed [1], [5]–[8]. CFD models are more computationally demanding than analytical ones, but are capable of handling complex geometries, require less assumptions, and can provide detailed information about heat transfer, mixing and combustion processes within the cookstove. Burnham-Slipper [5] developed a two dimensional axisymmetric steady state Reynolds Averaged Navier Stokes (RANS) model coupled with a pyrolysis sub-model, including combustion in the gas phase modeled by a single step reaction. The model considered the simple geometry of a cylinder as the riser with an aluminum plate on top to simulate the cooking surface. Heat transfer through conduction, convection and radiation was modeled, though radiation due to soot was neglected. The model was compared to temperature and heat transfer data from experiments. The model predicted burn rates and temperatures inside the stove for some cases but not for others, such as when the stove diameter, stove height and distance between the plate and body were changed. Miller-Lionberg [6] developed a three dimensional transient LES model with combustion modeled by a mixture fraction method and soot predicted by the Moss-Brookes model, along with heat transfer to the environment through convection, conduction and radiation. Inputs to the model were a realistic geometry of an improved rocket stove and fuel flow rates calculated at low and high firepower. The model predicted the overall heat transfer to the pot accurately for high firepower, but the low firepower case had an error of 29%. The heat transfer to the bottom of the pot was overpredicted, and the heat transfer to the side of the pot was predicted to be negative in both cases. CO and PM emissions were under-predicted by four and ten orders of magnitude, respectively. Wohlgemuth et al. [7] studied the effect of the gap between the pot and pot skirt using a axisymmetric RANS CFD model. Combustion was not modeled, and the velocity, temperature and turbulent intensity of the was specified when the gas exited the combustion chamber. The study suggests that there is an optimum gap distance between the pot and pot skirt for maximizing the thermal efficiency, and that insulating the pot skirt increases the efficiency of the stove. Bryden, et al. [8] used a graph-based genetic algorithm coupled with a three dimensional CFD model of a plancha stove to minimize the spatial temperature variations on the cooking surface of the stove by placing baffles in the flow.

While these models have advanced the state of the art, they have largely been developed independently with limited reference to earlier modeling efforts. They have also been validated and used for a limited number of (and often simple) geometries. Combustion has often been modeled inadequately, and heat transfer modeled without considering the presence of soot. The effect of the changing internal geometry of an improved stove, such as the shape of the cone deck, secondary air entrainment and baffles on the flow, combustion and turbulent mixing have not been studied. The underlying physics behind why certain configurations result in better emissions and thermal efficiencies has also not been adequately explored.

In this project, we developed a steady-state, two-dimensional axisymmetric RANS model to simulate the fluid flow, combustion, turbulence and heat transfer in a wood burning, natural draft rocket stove. Combustion was modeled by an 11 species, 21 step reaction mechanism using the finite laminar rate method. The model includes heat transfer by conduction, convection and radiation, including heat loss from the cookstove to the environment and heat radiated by the soot-laden gas. We examined the effect of various geometric parameters such as the pot support height, secondary air injection and the insertion of baffles on the excess air, primary air flow, secondary air flow, turbulent mixing and heat transfer to the pot. We predicted excess air in the stove as a function of firepower and find that it is many times the flow required to meet combustion stoichiometry requirements. We also found that secondary air entrainment by itself is not effectual in increasing mixing inside the cookstove, but is effective when coupled with a central baffle. Through this process we gained an understanding of the physics at work inside the cookstove, which can be used by stove designers to alter the flow field and temperature distribution inside the cookstove in order to enhance heat transfer to the pot and reduce emissions by increasing turbulence and mixing.

Computational Model

A schematic of the computational model is shown in Figure 12. Air enters from the primary air inlet at the bottom of the stove and wood volatiles are discharged uniformly from three toroidal fuel inlets. The wood volatiles and air mix in the combustion chamber, which is a cylindrical cavity of 100 mm diameter and 291 mm height, giving rise to flaming combustion. The riser provides a flow path above the combustion chamber. Secondary air is entrained into the riser 150 mm above the primary air inlet. The hot combustion gases flow towards the 280 mm diameter pot that is placed above the riser atop a conical-shaped cone deck. The cone deck serves as a gradual area expansion for the gas flow, to prevent flow separation, and directs flow over the bottom of the pot and out to the 340 mm diameter pot skirt. A pot skirt is an optional stove feature that directs hot combustion gases along the sides of the pot and improves heat transfer to the pot [7].

The fuel inlet is modeled as three conical rings that have the same surface area as the nominal four sticks of wood used in the experimental work. The flux rate of volatiles entering the computational domain is set to match the desired burn rate. The model does not provide a feedback mechanism from the flame to the fuel devolatilization process. The composition of wood volatiles is taken from Galgano et al. [9] with minor modifications, as shown in Table 1.

Species	CO	CO_2	H_2	H_2O
Mass Fraction	0.383	0.273	0.032	0.312

Table 1: Mass fraction of species in wood volatile mix

We solve the Reynolds-averaged conservation equations of mass, momentum, energy, and species transport. We model turbulence using the Realizable $k-\varepsilon$ turbulence model, which is a modified form of the standard two-equation $k-\varepsilon$ model [10]. The model solves transport equations for turbulent kinetic energy, k, and the turbulent dissipation rate, ε [11]. We close the momentum equation by calculating the turbulent eddy viscosity,

$$\mu_T = \rho C_\mu \frac{k^2}{\varepsilon} \tag{1}$$

from the turbulent kinetic energy k, the turbulent dissipation rate ε, the density ρ, and C_μ, a model parameter that is a function of the strain rate tensor, k, and ε [10]. The energy equation is closed by assuming a turbulent Prandtl number of 0.9 [11] .The specific heat at constant pressure of each species is assumed to vary as a polynomial function of temperature, while the specific heat of the mixture is a mass-weighted average of the specific heats of the individual species [12]. We compute the laminar dynamic viscosity using Sutherland's Law [13]. The molecular diffusivity of the mixture is calculated from the Schmidt number, assumed to be constant at 0.9, and the thermal conductivity from the Lewis number, assumed to be constant at 1.0 [14] [15]. We model radiation by solving the radiative transfer equation (RTE) by the discrete ordinates method, using the S_4 approximation [14]. While the presence of soot is important for heat transfer by radiation, we do not explicitly model the soot, instead

opting for the use of a uniform and constant absorption coefficient of the gas as a surrogate for soot radiation [7]. An increased absorption coefficient due to the presence of soot is accounted for by calibrating the model with experimental results. All surfaces are assumed to be black and the gas is assumed to be gray.

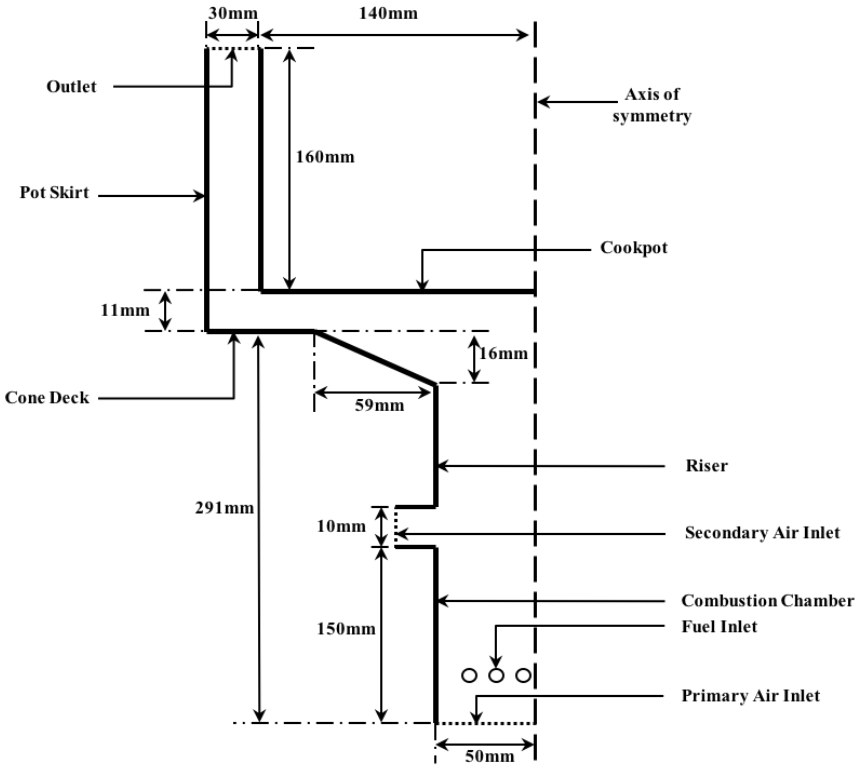

Figure 12. Schematic of axisymmetric computational model. Air enters from the primary and secondary air inlets; fuel enters from the conical-shaped fuel inlet. The flow exits at the outlet.

We model combustion with the laminar finite rate model, where reaction rates are determined by Arrhenius kinetic expressions [12]. The source term for each species transport equation is given by the Arrhenius expression for each reaction involving that specie in the chemical kinetic mechanism. We use the 11-species, 21-step reaction mechanism proposed by Hawkes et al [16]. Since the chemical mechanism does not include methane as a species, we convert the methane in the original composition to an equivalent amount of hydrogen on a heating value basis. We solve transport equations for each species, of the form,

$$\frac{\partial}{\partial t}(\rho Y_i) + \nabla \cdot (\rho \boldsymbol{U} Y_i - \boldsymbol{F_i}) = S_i \qquad (2)$$

where Y_i is the mass fraction of specie i, $\boldsymbol{U}$ is the velocity, $\boldsymbol{F_i}$ is the diffusion flux and S_i is the source term for species i.

The model requires boundary conditions for the inlets, outlet, and stove walls. The air at the inlet is entrained by natural convection and thus we specify atmospheric pressure and temperature (300 K) and a turbulent intensity of 7.5%. The fuel inlet is specified as a mass flow rate with the flux of volatiles set by the desired burn rate of 2 to 5 kW, which is consistent with burn rates in cookstove modeling literature, as well as those observed in the lab and field [3], [6], [17]. The boundary condition at outlet of the pot skirt is specified as atmospheric pressure. The cookpot is isothermal at the boiling point of water at atmospheric pressure (373 K). The combustion chamber, riser, cone deck, and pot skirt are modeled using a mixed convection, conduction and radiation boundary condition. By this procedure, a heat transfer coefficient for each of the boundaries mentioned above is calculated. This combined heat transfer coefficient includes the effect of the wall thickness, insulation thickness and convection and radiation from the outer body to the environment. The external heat transfer coefficients are calculated using standard heat transfer correlations [18].

The simulations are carried out using the STAR-CCM+ commercial software package using the finite volume method [13]. We use an unstructured polyhedral mesh selected after grid independence studies. Prism layers are added near the walls to adequately resolve the boundary layer in order to eliminate the need of wall functions in the turbulence model and accurately predict the heat transfer to the walls and the pot.

For the purpose of calibrating the model to account for the presence of soot, we measure gas temperatures in the gap between the pot and the pot skirt at five locations at 1.5, 5.5, 10, 14, and 17 cm from the bottom of the pot skirt in a vertical line, as shown in Figure 3(B). Type-K thermocouples (3859K44, McMaster-Carr, Elmhurst, IL) are used and thermally isolated from the skirt using fiberglass insulation wrapped around the probes (while keeping the junctions exposed) to prevent contact with the pot skirt. Tests are performed with the thermocouples located at the front, side, and back of the cookstove, with the location varied by rotating the pot skirt and thermocouples. The measured temperatures are averaged over short time periods where the average firepower is close to 4 kW.

The mean absorption coefficient for a luminous flame is given by $\kappa = 3.6\, cT_m/c_2$, where κ is the mean absorption coefficient in m^{-1}, T_m is the temperature in Kelvin, c_2 is the second constant of radiation, equal to $1.4388 \times 10^{-2}\ mK$ [19]. The constant C is defined as,

$$c = 36\pi f_v \frac{n^2 k}{[n^2 - (nk)^2 + 2]^2 + 4n^2k^2} \tag{4}$$

where n and k are the refractive and absorptive indices of refraction of the soot particles, respectively, and f_v is the soot volume fraction. The values of n and k are calculated assuming a representative temperature of 1000 K, at which temperature the peak wavelength of radiation by Wien's law is approximately 3 μm. At this wavelength, the values of n and k are 2.5 and 1.3, respectively [7]. Soot volume fractions in turbulent hydrocarbon flames range from 3×10^{-8} to 10^{-5} [14], which results in absorption coefficients in the range 0.03 m^{-1} to 11 m^{-1}. In real flames the absorption coefficient varies spatially and depends on the temperature and soot volume fraction. Since we do not directly model soot, and thus do not know the values of the soot volume fraction, we instead account for the radiation heat transfer due to soot by employing an artificially high value of the gas absorption coefficient [7]. In this approach, the model is calibrated by adjusting the spatially uniform mean absorption coefficient

We use the model to examine the relationship between firepower and airflow rate. Figure 13(A) shows a plot of the computed total, primary, and secondary air mass flow rates, as well as the experimentally measured total mass flow rate as a function of firepower. The experimental mass flow rate is calculated from the measured excess air and firepower. Somewhat counterintuitively, the total mass flow rate remains nearly constant with firepower, as observed in both measurement and computation. This is due to the competing effects of decreasing density and increasing volume flow rates due to increased draft. Fuel consumption increases linearly with firepower, which results in higher gas temperatures. This leads to a larger draft, and therefore, an increased volume flow rate through the outlet. However, the increased temperature also results in lowered density, which leads to a relatively constant mass flow rate over a wide range of firepowers. This effect of having a relatively constant mass flow rate over this range of firepowers is also observed in the predictions made by Agenbroad et al [3], for which they provide a similar reasoning. From the figure, we also observe that the primary air flow rate decreases slightly as firepower increases, while the secondary air flow rate increases slightly with increasing firepower. Figure 5(B) shows a plot of the excess air through the stove as a function of firepower for the CFD model and experiments. A constant air mass flow rate results in a lower excess air with increasing firepower, since more fuel is being injected with no change in airflow. At a low firepower of 2 kW, the amount of air present in the system is in excess of ten times what is required for complete combustion. At the highest fire power examined (5 kW), the excess air is still more than three times greater than what is required. Some excess air is recommended to enhance mixing and avoid rich combustion that could result in unwanted soot production [20]. Conversely, too much cool air flowing through the stove cools the combustion gases and can diminish heat transfer to the pot and degrade the thermal efficiency, as was also hypothesized by Baldwin [2].

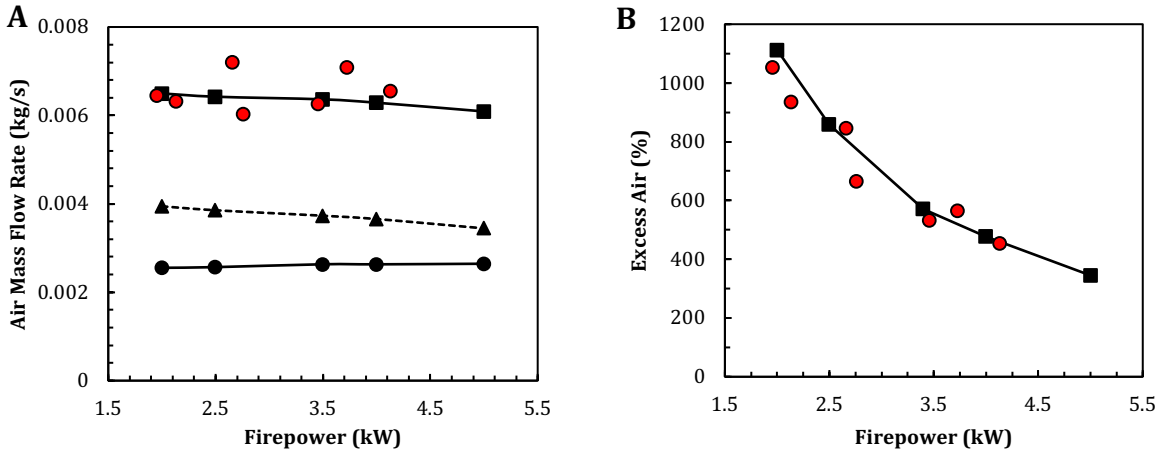

Figure 13. (A) Plot of airflow rate as a function of firepower. The circular red markers are experimental results. The square, triangular, and circular black markers are the total, primary and secondary air mass flow rates predicted by the CFD model, respectively. (B) Plot of air-fuel ratio as a function of firepower of cookstove. The circular markers are experimental results and the square markers are results obtained from the CFD model

We examine the relationship between excess air and thermal efficiency by varying the pot support height. It is known, and we have experimentally observed, that the pot support height strongly impacts the excess air and stove thermal efficiency [2][5]. Using the computational model, we vary the pot support height from 7 mm to 15 mm for a constant firepower of 4 kW, and extract the total air mass flow rate and excess air ratio as shown in Figure 14(A). The data shows the excess air ratio and airflow rate increase and appears to asymptote to a constant value as the pot support height increases. We hypothesize that the lower excess air is due to obstruction to the flow (pressure drop) created by the shorter pot support heights. As we increase the pot support height, obstruction to the flow is reduced and the excess air increases. In this case, we expect the excess air ratio and airflow rate curves to have the same shape since the firepower is held constant. Both curves appear to asymptote to a constant value as the pot support height increases since the effect of the pot on the airflow will reduce as the pot is moved further away from the cookstove.

Figure 14(B) shows the stove efficiency as a function of pot support height. We define the stove efficiency as the percentage of the total heating value delivered to the pot of water. We observe that the efficiency is 35% for a pot support height of 7 mm and reduces to 30% as the pot support height is increased to 15 mm. The efficiency decreases with pot support height because airflow through the cookstove increases as the pot support height is increased which results in a lower bulk gas temperature and less heat transferred to the pot. This result is similar to that of Baldwin [2], who predicted that narrower gaps in the cookstove lead to higher heat transfer to the pot. However, further reducing the pot support height would increasingly reduce the airflow rate until combustion can no longer be sustained.

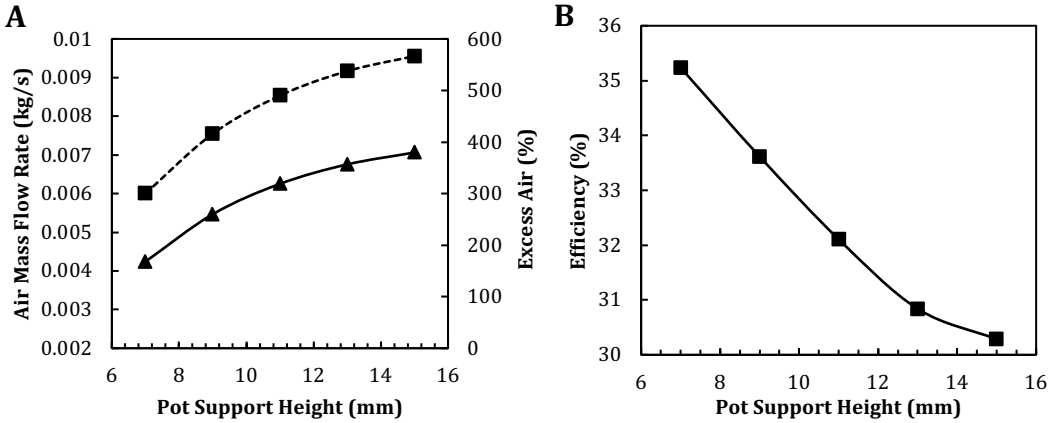

Figure 14. (A) Air mass flow rate (solid line with triangles) and excess air (dashed line with squares) as a function of pot support height. (B) Heat transfer efficiency to the pot as a function of pot support height.

Another method of reducing the excess air in a cookstove is the placement of a central baffle in the riser. Intuitively, we understand that the baffle will cause a pressure drop, causing a reduction in airflow. We examine the effect of baffle size on the airflow rate, thermal efficiency and mixing. The OH mass fraction, temperature distribution and the turbulent kinetic energy inside a cookstove with secondary air and with and without a central baffle are show in Figure 15. Figures 15(A) and 15(C) show the computed OH mass fraction and temperature distribution inside the cookstove with secondary air injection. The OH radical is highly reactive and short-lived, and hence can be used to track the position of the flame front [12]. The flame is a diffusion flame and can be seen as a thin sheet of high OH concentration that sits at the intersection of the air and fuel in Figure 15(A). Note that the flame front denoted by high OH concentration is also the hottest part of the flame. Figure 15(C) shows the temperature distribution in the stove which varies from 1800 K in the flame front to 300 K at the air inlet. A zone of cold air is seen around the flame, which does not contribute to the combustion, but mixes with the burned gases further downstream and reduces the bulk gas temperature, which leads to a reduction in heat transfer to the pot. The cold air entering from the secondary air inlet does not penetrate the main flow and moves up along the riser wall. The turbulent kinetic energy distribution with secondary air, shown in Figure 15(E) shows very little turbulence in the region within the flame sheet. This evidences the secondary air contributing minimally to mixing inside the stove.

Figures 15(B), (D) and (E) show the OH mass fraction, temperature distribution, and turbulent kinetic energy distribution inside the cookstove with secondary air and a central baffle blocking 45% of the riser area. When we add the baffle to the stove the temperature distribution is more uniform in the region above the riser and the turbulent kinetic energy is greater, suggesting enhanced mixing in the upper part of the riser. The presence of the baffle causes the flame to break up, as seen in the temperature distribution and OH mass fraction plots. The presence of the baffle also results in a reduction in the primary airflow rate, from 0.0034 kg/g to 0.0025 kg/s due to the flow obstruction caused by the baffle. The secondary airflow rate remains approximately the same when the baffle is present. Together, the baffle and secondary air flow results in better mixing downstream of the baffle, as is seen from the more uniform temperature distribution and greater turbulent energy. Higher temperatures and increased turbulent mixing have been linked to lower PM emissions in cookstoves [21].

Figure 16(A) shows plots of primary, secondary and total air mass flow rates as a function of the percentage of riser area blocked by the central baffle, at a constant firepower of 4 kW. When no baffle is present, the airflow rate is nearly evenly divided between the primary and secondary air. The primary air flow rate decreases with increasing baffle size, since the baffle obstructs the primary air. At 75% riser area blockage, only 25% of the total airflow is contributed by the primary air. Figure 16 (B) shows the effect of increasing baffle size on the stove efficiency. The stove efficiency reduces slightly as the baffle size is increased. This is in direct contrast to Figure 14, which shows that reducing the pot support height (and hence, the total airflow) increases the thermal efficiency. This can be explained as follows: When flow is blocked by a central baffle, though the reduced airflow rate leads to higher bulk temperatures, more heat is absorbed by the riser walls and cone deck due to better mixing. When flow is reduced by some other means which does not increase the mixing (reducing the pot support height, for example), the zone of cold air surrounding the flame acts as an insulator, leading to a lower amount of heat absorbed by the cone deck and riser. This is why reducing the airflow in one configuration leads to a higher thermal efficiency, but a higher one in the other. This also supports the hypothesis that merely reducing the airflow rate is not sufficient to increase the efficiency; the mechanism of airflow blockage is also important.

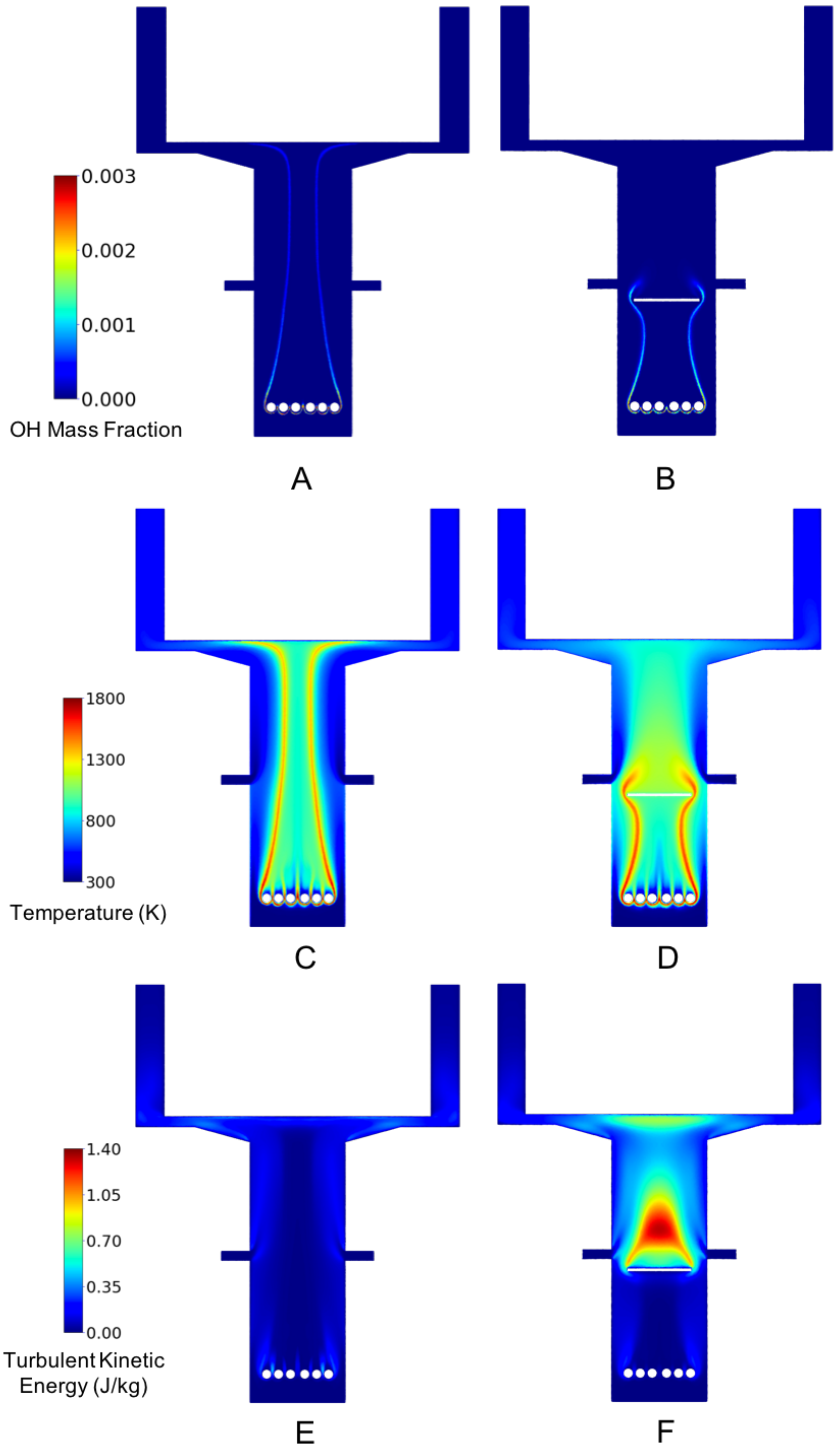

Figure 15. (A) Computed OH mass fraction with secondary air. (B) Computed OH mass fraction with secondary air and central baffle blocking 45% of riser area. (C) Computed temperature distribution with secondary air. (D) Computed temperature distribution with secondary air and central baffle blocking 45% of riser area. (E) Computed turbulent kinetic energy with secondary air. (F) Computed turbulent kinetic energy with secondary air and central baffle blocking 45% of riser area.

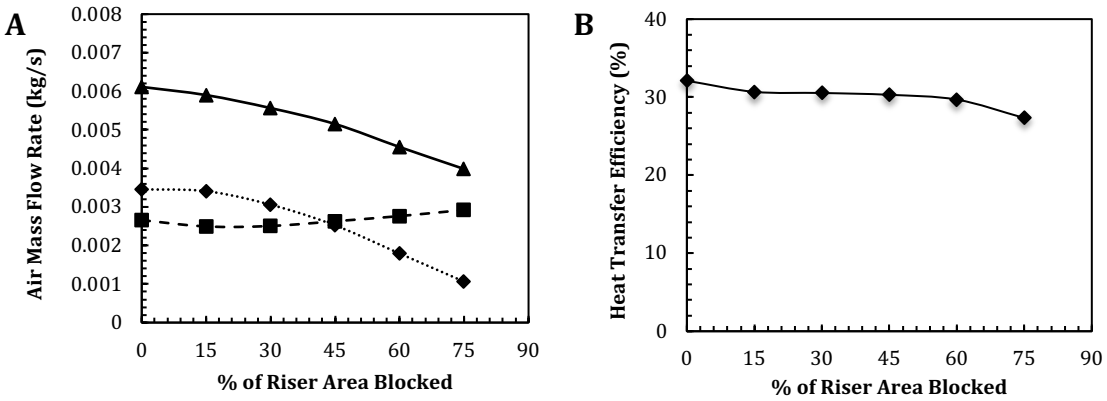

Figure 16. (A) Primary (dotted line, diamond), secondary (dashed line, squares), and total (solid line with triangles) airflow rate as a function of riser area blocked by central baffle. The total airflow reduces as the size of the baffle is increased. The contribution of primary air reduces, and that of secondary air increases with increasing baffle size. (B) Stove efficiency as a function of riser area blocked by central baffle. The efficiency decreases slightly as baffle size increases.

Next, we examine the effect of the shape of the cone deck on the thermal efficiency and airflow rate. The cone deck is the part of the cookstove placed on top of the riser. It serves as a gradual area expansion for the gas flow, which mitigates the effects of flow separation and directs flow under the bottom of the pot. A sample cone deck and its placement on a cookstove is shown in Figures 17(a) and (b).

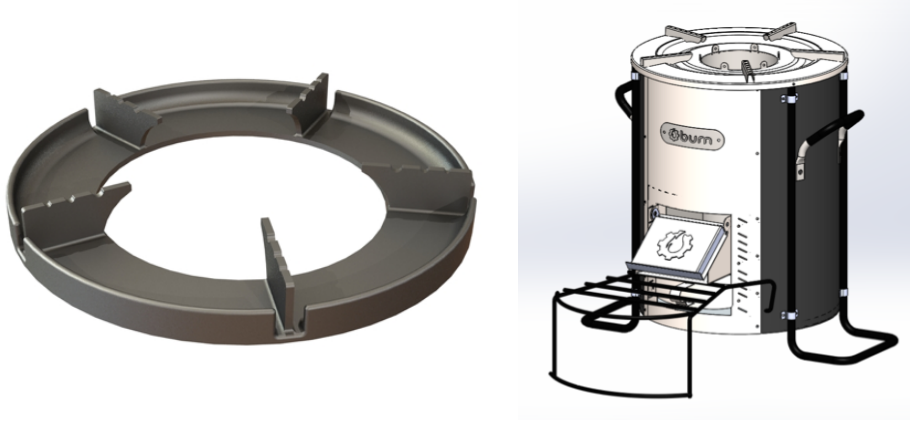

Figure 17. (a) Example of a cone deck. (b) Position of cone deck on a cookstove.

Conventional wisdom states that for optimal heat transfer to the pot, the cross-sectional area of the flow path throughout the cookstove should be constant, including the flow area over the cone deck [22], [23]. To examine the veracity of this guideline, we present the results of varying the shape of the cone deck on performance parameters such as thermal efficiency and airflow rate. We define the cone deck using three geometric parameters, as shown in Figure 18: the horizontal distance from the centerline to the far end of the slanted region, *X*, the vertical distance between the top and bottom of the slanted region, *Y*, and the height of the pot supports. A total of 36 cone decks are modeled, with *X* values of 79 mm, 108 mm, 138 mm and 168 mm, *Y* values of 8 mm, 16 mm, and 24 mm and the pot support height values of 7 mm, 9 mm, and 11 mm. Each possible combination of *X*, *Y* and the pot support height is modeled for a constant firepower of 4 kW.

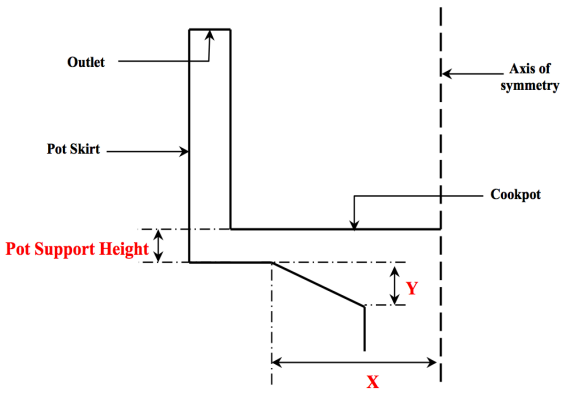

Figure 18. Geometric parameters defining cone deck shape.

In order to understand the effect of the shape of the cone deck on the thermal efficiency, we plot the thermal efficiency of the cookstove as a function of the airflow rate through the cookstove, shown in Figure 19(a). We observe that the efficiency of the cookstove for differing cone deck configurations is highly correlated with the air flow rate through the cookstove. This data suggests the shape of the cone deck only controls the flow of air through the cookstove, as each configuration has a different pressure drop associated with it. We also observe that the efficiency drops as the airflow increases. As with the pot support height analysis, we hypothesize that this is due to a decrease in the bulk temperature of the gas, which reduces heat transfer to the cookpot. Figure 19(b), shows the averaged gas temperature at the riser outlet as a function of air mass flow rate, supports this hypothesis. The bulk temperature reduces as airflow increases.

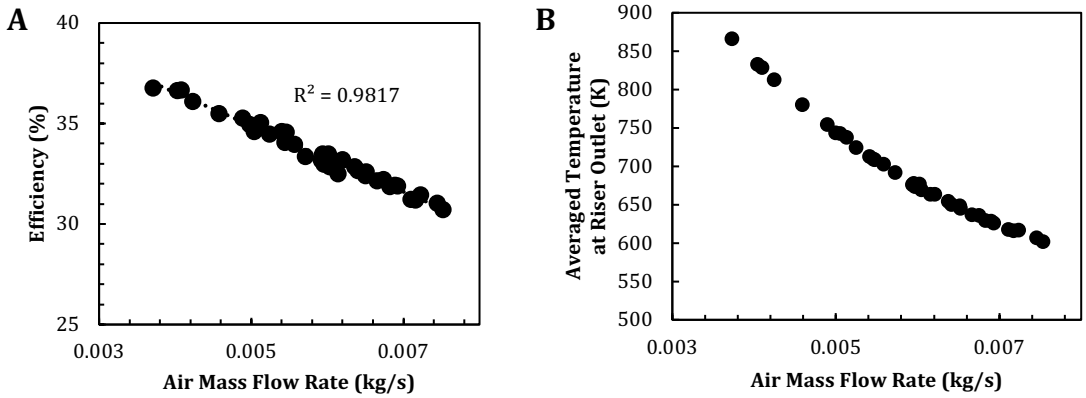

Figure 19. Predicted thermal efficiencies and bulk temperatures for various cone decks configurations (a) Thermal efficiency as a function of air mass flow rate. Each point represents a specific cone deck configuration. The dotted line is a linear trend line. (b) Mass-averaged temperature at the mouth of the riser as a function of air mass flow rate. Each point represents a specific cone deck configuration.

We examine the relationship of airflow rate and efficiency further, by comparing the pressure drop across the cookstove for different baffle and cone deck configurations. Figure 20(a) shows the predicted mass flow rates through the cookstove as a function of the pressure drop through the cookstove for baffle and cone deck configurations. As expected, both sets of data exhibit the same linear trend, and are highly correlated. The thermal efficiency for the baffle and cone deck configurations, on the other hand, does not correlate well, as shown in Figure 20(b). This further supports the hypothesis that merely reducing excess air might not lead to an increase in thermal efficiency; the location where flow is obstructed is important, and needs careful consideration.

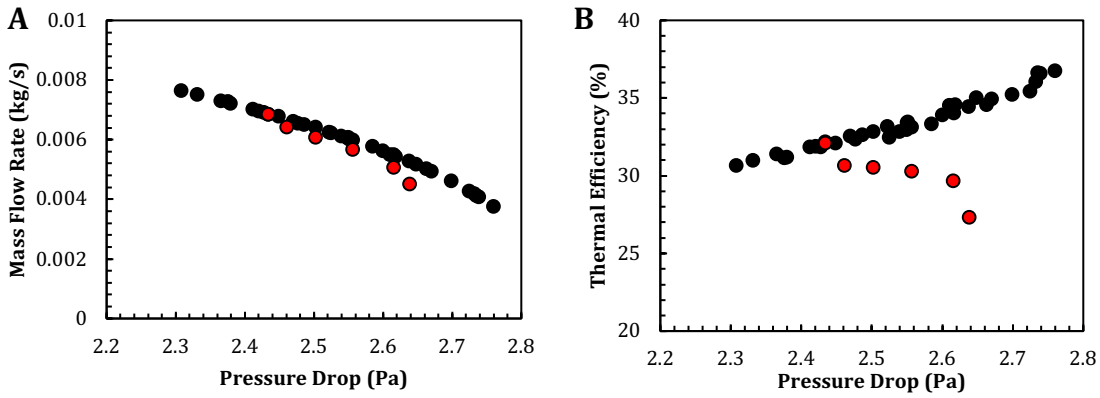

Figure 20. Predicted mass flow rates and thermal efficiencies for various cone deck configurations and baffle sizes. Each point represents a specific cone deck/baffle configuration. Black markers represent cone deck configurations and red markers represent baffle configurations. (a) Mass flow rate through the cookstove as a function of pressure drop. (b) Thermal efficiency of cookstove as a function of pressure drop.

Based on the results of this study, two cone decks were built and tested. The experimental and numerically predicted results are shown in Figure 21. The X value for both cone decks was 108 mm, while the Y values were 10 mm and 20 mm. Both cone decks were tested at pot support heights of 9 mm and 11 mm at an average firepower of 3.5 kW. The comparison of the results of experiments and numerical simulations for each configuration. The configurations are as follows:

- Configuration 1: X = 108 mm, Y = 20 mm, Pot support height = 11 mm
- Configuration 2: X = 108 mm, Y = 10 mm, Pot support height = 11 mm
- Configuration 3: X = 108 mm, Y = 10 mm, Pot support height = 9 mm

The model's predictions of thermal efficiency for each configuration is quite close to the experimental results. Configuration 3 gives the best performance, with an average thermal efficiency of 35.9%, an increase of 6.8% over Configuration 1 and 5.5% over Configuration 2.

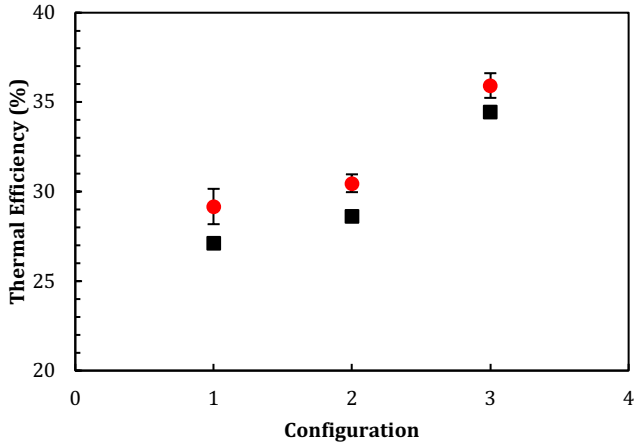

Figure 21. Thermal efficiency of three cone deck configurations. The red markers are experimental results with 90% confidence intervals and the black markers are numerical results. Configuration 1 is a cone deck with X = 108 mm, Y = 20 mm, and pot support height = 11 mm. Configuration 2 is a cone deck with X = 108 mm, Y = 10 mm and pot support height = 11 mm. Configuration 3 is a cone deck with X = 108 mm, Y = 10 mm and pot support height = 9 mm.

A two dimensional, steady state, axisymmetric CFD study was performed on a configuration representing a wood burning, natural draft rocket cookstove. A Reynolds Averaged Navier Stokes approach was used to model the cookstove. Combustion was modeled by an 11 species, 21 reaction chemical kinetic mechanism. Heat transfer from the soot-laden gas to the cookpot and stove body, and from the stove body to the environment by all three modes was also included in the analysis. The model was calibrated and validated against experimental data and was found to accurately predict the excess air through the cookstove and the temperature distribution between the pot and pot skirt. The excess air in the cookstove was found to be several times stoichiometric air for almost every configuration, except those where the flow was severely constricted due to a narrow passage. It is in the interest of stove designers to reduce the excess air, which acts as a diluent and reduces the bulk temperature inside the cookstove.

Various geometric parameters such as the height of the pot supports, secondary air entrainment, central baffles of various sizes placed within the riser and cone deck shape were analyzed. The pot support height was found to have a strong effect on the excess air ratio as well as the stove efficiency, consistent with previously published literature. Lower pot support heights were found to provide a lower excess air ratio and higher stove efficiency, provided that the firepower is maintained relatively constant. However, a further reduction in the pot support height would lead to a lowered efficiency, due to a reduction in the airflow rate, which would lead to there being not enough air to sustain combustion. This effect is not captured by our model. Energy efficient designs will need to optimize the height of the pot supports such that the design allows a large enough airflow rate.

Secondary air entrainment by itself was found to be ineffectual in increasing the mixing or heat transfer efficiency in the cookstove. In order to increase the mixing and cut down on the excess air, a central baffles blocking between 0 and 75% of the area of the riser were introduced into the flow via simulation. We found that secondary air entrainment, when used in conjunction with a central baffle, led to a decrease in the total airflow rate and an increase in turbulent mixing downstream of the baffle, which led to better mixing, which could reduce $PM_{2.5}$ emissions. The central baffle adversely affects stove efficiency, with larger baffle sizes leading to lower efficiencies despite lower air flow rates. This was due to larger heat losses from the cone deck and riser walls because of a more uniform temperature profile.

The effect of the shape of the cone deck on the thermal efficiency was investigated by modeling 36 different cone deck configurations. The results suggest that the shape of the cone deck controls the airflow rate through the cookstove. A reduction in airflow causes the bulk temperature to increase, which leads to an increase in thermal efficiency. Based on these findings, three cone deck configurations were experimentally tested. The experimental results closely matched the predicted ones.

The pot support height, baffle and cone deck were all shown to reduce the amount of air flowing through the cookstove, but their effects on thermal efficiency were varied, such that a similar air mass flow rate for different configurations resulted in different stove efficiencies. This suggests that merely reducing the airflow is not a sufficient condition to increasing stove efficiency; stove designers also need to think about the location of flow obstructions and the effects of mixing within the cookstove.

3.3 Iterative Design

Improving the conversion of biomass energy while reducing emissions has been the aspiration of stove development programs for some time, with performance aspirations of 90% PM emissions reduction and 50% fuel saving over traditional cooking technology such as the three stone fire. To guide the design and development of cookstove, a gathering of a broad international array of household energy experts and stakeholders, who drafted and agreed upon performance standards, including the International Organization for Standardization (ISO) International Workshop Agreement (IWA) 11:2012 (IWA 11:2012): Guidelines for Evaluating Cookstove Performance (ISO 2012). IWA 11:2012, provides quantitative grading of cookstove performance for 1) fuel efficiency, 2) total emissions, 3) indoor emissions, and 4) safety, under standard testing protocols, such as the Water Boil Test (WBT) or the Kitchen Performance Test (KPT), outlined in “Tiers of Performance”. Tiers span from 0-4, with tier 0 performance equivalent to a TSF and tier 4 performance meeting aspirational goals that satisfy WHO guidelines.

In this project we had the original goal of developing a Tier 4, wood burning natural draft production stove. Soon after the project began, we modified our approach to achieve more realistic goals. Our first goal was to make a prototype natural draft rockets that achieved Tier 4 metrics but may not have the usability, features, and

durability of a production stove. This high-performance stove would serve to teach strategies to achieve high performance without the typical boundaries of a production stove that would be delivered to users. Next, we aimed to take these lessons and develop a production stove prototype that was acceptable to users and could be mass produced. This stove may not perform as well as the Tier 4 concept stove, but it would be acceptable to users and achieve the other usability metrics as well as be high performing compared to traditional fires and commercially available improved cookstove. In this section we describe the tier 4 concept stove called the "Tallboy" as well at the production stove prototype the "35B."

The Tallboy Tier 4 Concept Stove

One of our goals was to design a natural draft cookstove that obtained ISO-IWA 11:2012 tier 4 ranking for all calculated metrics using the WBT protocol. The most difficult of these metrics to achieve is a thermal efficiency above 45%, and PM emissions rate below 2 mg-min^{-1}.

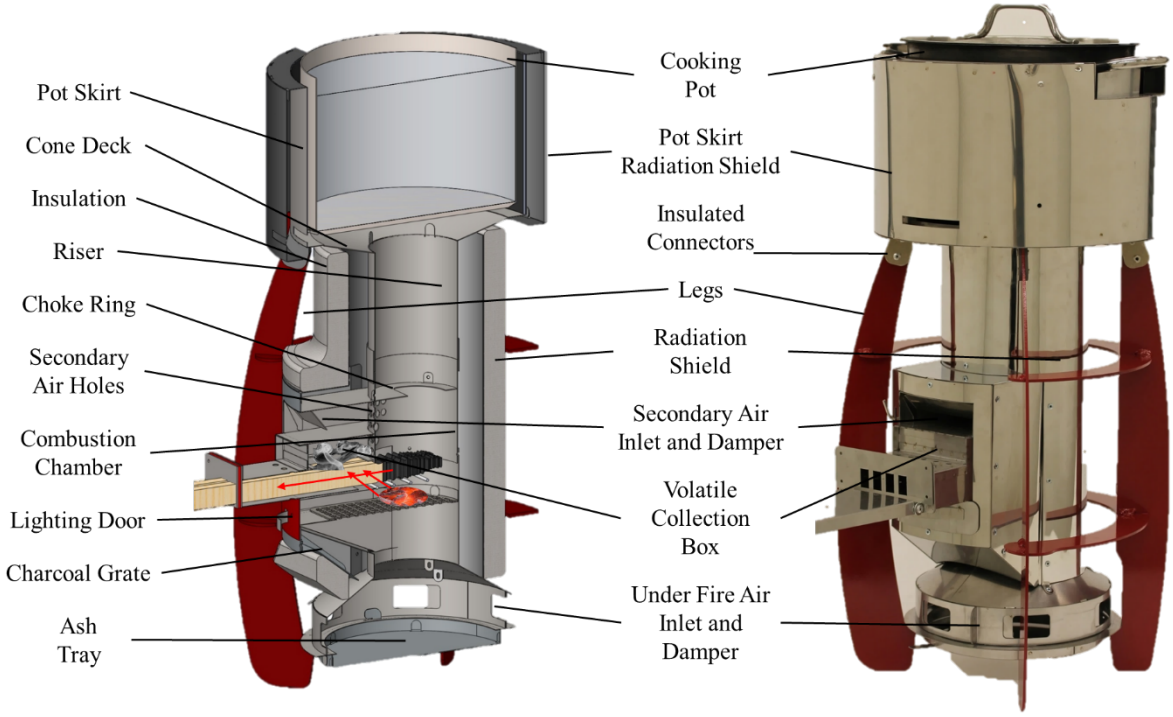

Figure 22. Cross sectional view of the Tallboy stove design, identifying interior stove components and stages of gasification (1-Drying, 2-Pyrolysis, 3-Combustion, 4-Char oxidation), red arrow show heat transferred to non-flaming regions of wood from char radiation and conduction from the hot flaming ends (A), and an image of the uninsulated prototype stove identifying exterior stove elements (B).

Figure 22 shows both a rendered drawing and an image of the Tallboy stove. The onset of gasification occurs in the feed tunnel where heat conducted from the hotter portions of wood elevates the wood temperature past the saturation temperature. The wood enters the feed tunnel and heat from the flame radiates to the wood feed and dries the wood as well as releases volatile compounds. The wood fuel is fed into the feed tunnel through a face plate where the opening dimensions were designed to match the dimensions of the sticks of wood, eliminating air flow through the feed tunnel. Reducing the air flow through the feed tunnel allows us to release the volatile combustion gases without combustion. The volatile gases can then be recaptured and burned in the gas phase when injected into the combustion chamber. Limiting the total air flow is valuable because air in excess

of that what is required for combustion can lower the average gas temperature in the stove and reduce the stoves thermal efficiency. Minimizing excess air is beneficial for heat transfer, however, restricting air flow below the stoichiometric threshold, will cause incomplete combustion, and higher carbon monoxide and PM emissions. Incorporating dampers into the design allows the user to tune the air flow rate, so combustion temperatures are at their maximum, and the total flow rate is above the stoichiometric limit. Separating air flow is commonly called staging, which has many benefits in the design of we are able to primary (under fire) and secondary air into the design.

Once in the feed tunnel, the first stage of gasification begins where heat the wood starts to dry, initiating the first stage of gasifcation. Wood below the volatile collection box receives radiative heat from the charcoal bed as well as conductive heat from the flaming ends of the stick, initiating pyrolysis. In an oxygen depleted environment, we increase the wood temperature which initiates pyrolysis through the release of volatile gas. Volatiles that are emitted are captured in the volatile collection box and injected into the lower part of the riser where they combust with the regulated secondary air. An axisymmetric choke ring is used to shorten the mixing length of secondary air with the fuel.

To reduce stove storage all interior stove walls are made out of light weight sheet metal. Radiative losses to environment are mitigated by low emissivity (highly polished) exterior stove walls. A pot skirt and fins on the pot are included to increase heat transfer to the pot. Radiation shields, insulation, and minimal insulated contact points are used to minimize energy pathways to the stove outer body.

Figure 23 shows the WBT performance metrics for the Tallboy, the Jetter baseline averages of wood burning rocket stoves, and UW baseline averages of wood burning rocket stoves. For all metrics the Tall Boy achieved tier 4 standards. A low thermal mass stove which includes an insulated pot skirt, a finned pot, low emissivity outer body, and radiation shield/fiber glass insulation reduces the amount of fuel required to complete cooking task. High power PM (mg/MJ_D) was reduced by nearly an order of magnitude and indoor PM emissions (mg/min) was reduced by over an order of magnitude when compared to the other stove designs.

The two most difficult ISO metrics to reach at thermal efficiency and PM emissions rates. Figure 24 shows a plot of efficiency versus PM emissions for several commercial stoves, average stove performance, as well as the Tallboy stove. In this figure it is advantageous to be in the lower right hand quarter where PM emissions are low and efficiencies are large.

Overall, we learned from the Tallboy stove that high efficiency performance can best be obtained by making a stove with low thermal mass, good insulation from the environment, and reducing excess air into the stove. If thermal mass is high than the heat of combustion goes to heating up stove components rather than to the pot. Good insulation reduces heat loss to the environment. Limiting excess air ensures that air in excess of that which is required to oxidize wood volatiles and mix the fuel and oxidizer generally lowers the average gas temperature in the flame. Lower average gas temperatures slow heat transfer and result in lower efficiencies. We also learned that high temperature components can best be insulated by radiation shields rather than solid insulation. We learned that heterogenous combustion can result in high PM production and that it is advantageous to burn the wood volatiles in the gas phase. We showed that a lower secondary grate can create two combustion zones: one for the wood and a lower one for char; and that these two zones have different optimal air flow requirements. We also learned that a choke ring and secondary air holes can reduce the PM and increase efficiency in the stove, but poorly placed ones can negatively impact performance. We use these lessons learned as well as the user research to design a clean burning and efficient stove that meets the needs and aspirations of East African cooks.

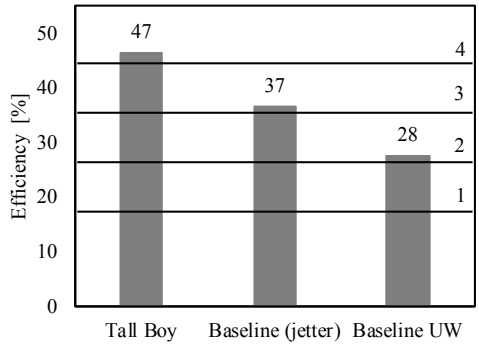

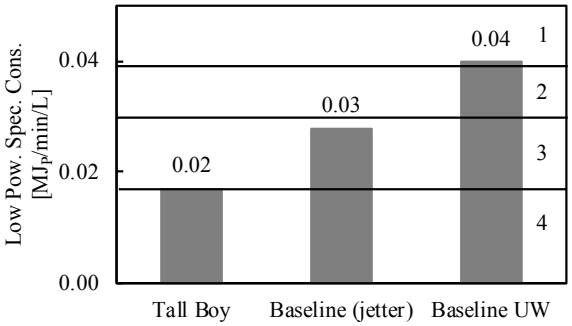

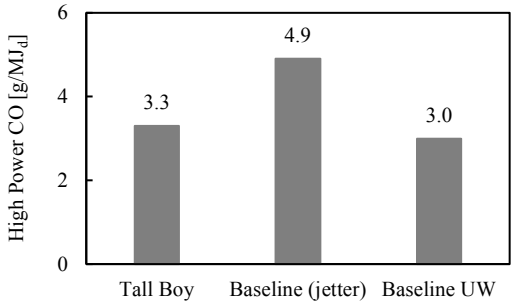

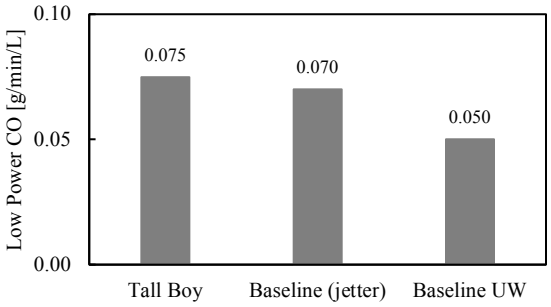

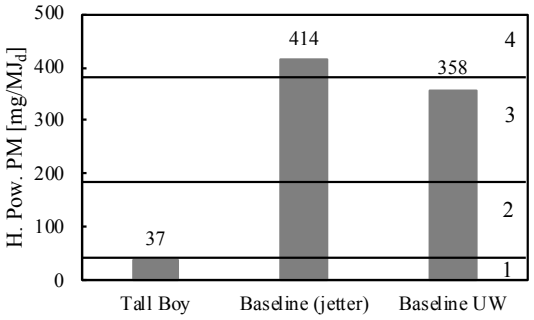

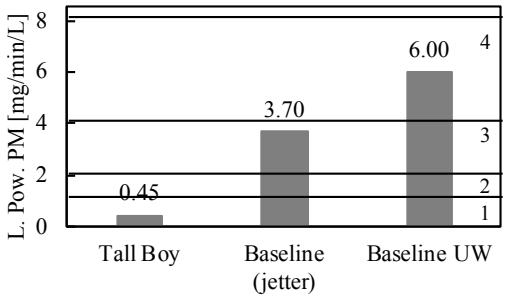

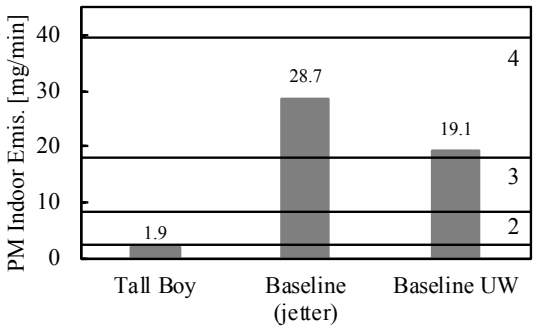

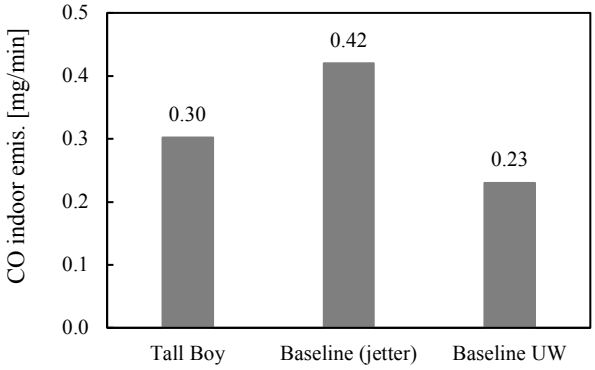

Figure 23(a-g). WBT metric results for the Tallboy. Regions listed by numeric values separated by lines on plots illustrate Tiers (1-4). If no lines present all stoves achieved tier 4 with maximum tier value listed in subfigure caption. The baseline Jetter results are the average wood burning rocket stoves from Jetter et al. [24]. The baseline UW results are average measurements obtained from four commercially available stoves in the UW lab.

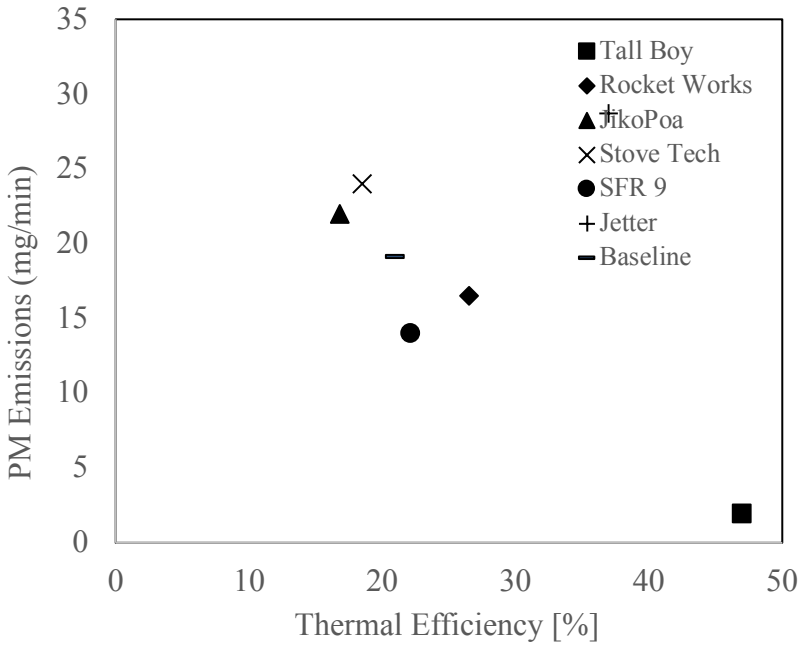

Figure 24. Map of thermal efficiency versus PM emissions for several typical rocket stoves as well as the tier 4 Tallboy stove. High performance stoves should demonstrate low PM emissions and high thermal efficiency (lower right).

Production Prototype 35

The goal for the SFR 35 development was to produce an all Tier 3 performing natural draft rocket stove using design ideas and lessons learned from the development of the better performing, but impractical, Tier 4 Tallboy prototype. The SFR 35 should be easily manufactured and a practical design that could be phased into production by BURN within the next year if the design proved itself to be a good performer in the field during a series of field tests in Kenya. The 35 stove design includes a radiation shield around the combustion chamber and riser, secondary air holes, a choke ring, a swing gate, and a lower grate, all learned from the Tallboy development. Air in the stove is fed below the grate through primary air as well as through preheated secondary air holes below the choke ring.

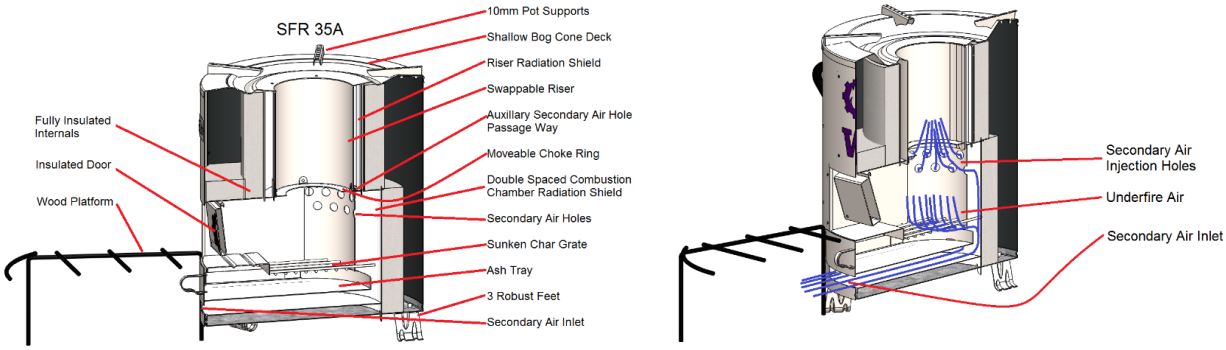

Figure 25. Cross sectional views for the general G35 series design. (Left) SFR 35A design. (Right) Secondary and under-fire air flow path.

Radiation shield gap is an important parameter impacting stove performance. If the gap is too large then natural convective currents develop it the gap and increase heat transfer. If the gap is too small then there is significant conduction. Secondary air flows through the lower part of the radiation shield so small gaps also

reduces the amount of secondary air. Stove height effects stove performance in numerous ways. The primary effect of the height is the induced natural draft. Another important factor is the distance between the fuel and pot which will play a role in the fire power required for the flame to impact on the pot. When the flame impacts the cold pot the flame is quenched which can increase particulate emissions. We also investigated the effect of secondary air hold pattern and injection location. Secondary air in the current design is used to improve the combustion efficiency as well as cool down combustion chamber. As shown in previous quarterly reports, the use of secondary air can reduce the combustion chamber temperature upwards of 150C. Eleven unique combinations were tested shown below in Figure 26.

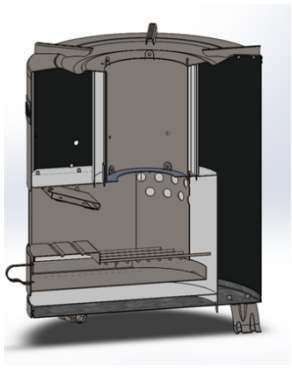

Baseline: None

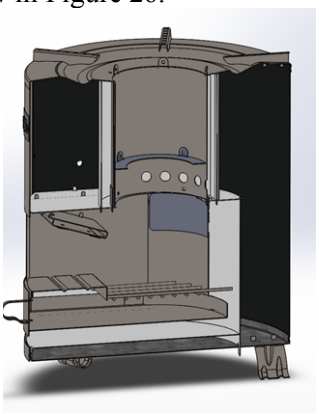

SA Blocked in CC + Riser Holes: Top Choke Ring

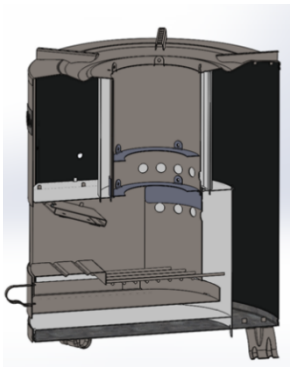

Top Holes Blocked in CC + Riser Holes: Two Choke Rings

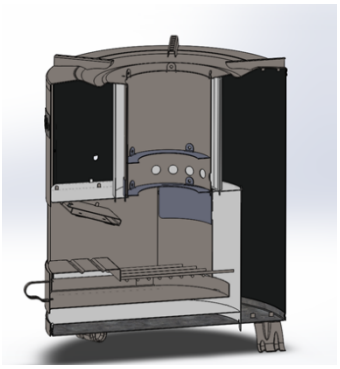

SA blocked in CC + Riser Holes: Double Choke Ring

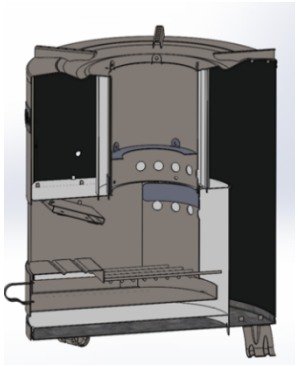

Top Holes Blocked in CC + Riser Holes: Top Choke Ring

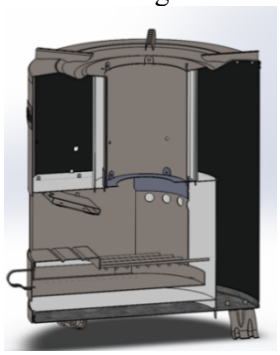

Baseline: Top Blocked

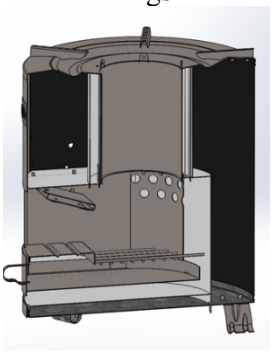

Baseline: No Choke Ring

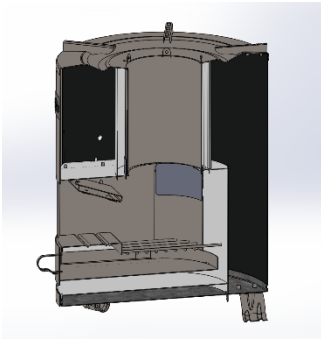

Baseline: No Choke Ring No SA

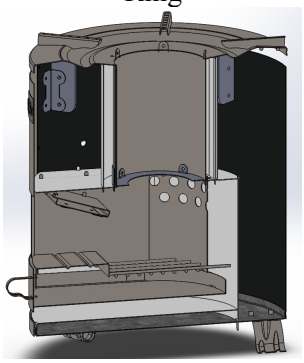

Baseline + No Cone Deck Contact Conduction

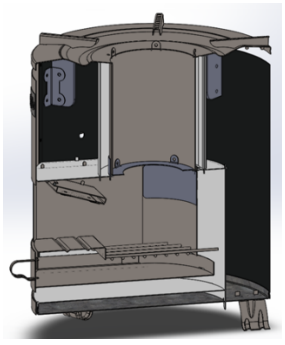

No Cone Deck Contact Conduction + No SA

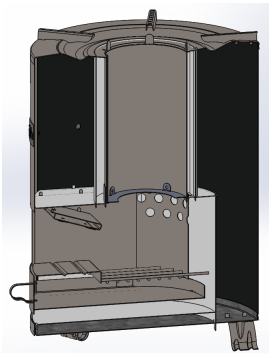

Baseline + Tall Body (+5cm)

Figure 26. Secondary air and choke ring geometries tested on the G35 stove.
SA = secondary air, CC = combustion chamber**

A great deal of work has gone into the design of a boil over gutter, which in the event of water boiling out the pot the boil over gutter acts as a reservoir for boiling water capturing it before it can enter the riser or combustion chamber. We tested three different BOG designs in combination with various pot support heights to investigate which design provided the greatest increases in efficiency and reduction in PM.

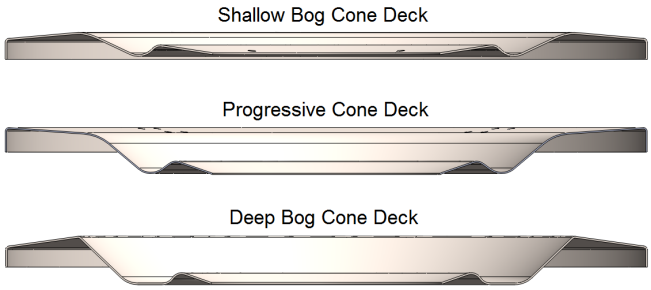

Figure 27. Three different BOG designs tested on the 35 series stoves.

Results were obtained using both the IWA water boil test as well as fire power sweeps testing procedure. Fire power sweeps allows for rapid analysis of the effect of operating fire power on PM production for different stove designs. The shortest stove tested was the G32J, which is 5cm shorter than the G35A and 10cm shorter than the G35A tall body. Initially all stoves were tested with 9 mm pot supports heights and a shallow BOG, the G35A was also tested using the deep bog. Plots of PM production (mg/min) versus fire power (kW) for three different stove heights shows that PM is reduced by increasing stove height and by using the deep BOG. The bottom plot compares all three BOG designs confirming that the deep BOG designs has the lowest PM emissions rates for all three designs.

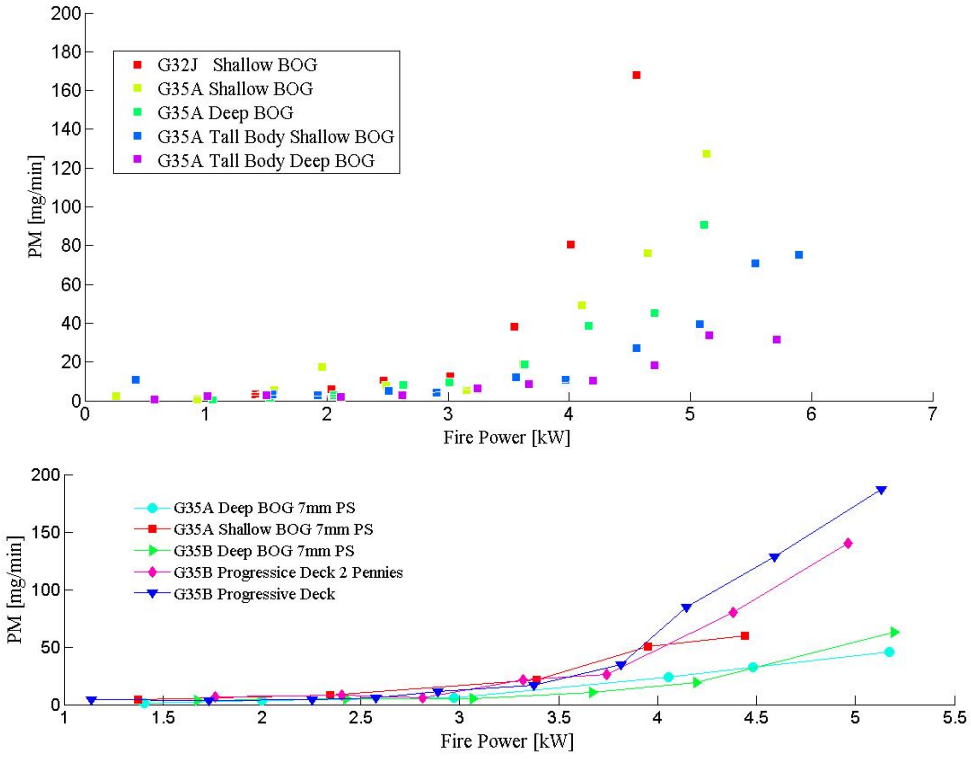

Figure 28. Fire Power Sweeps plot of PM emissions rate vs fire power. (Top) Three different stove heights and 2 different BOG designs. (Bottom) Two different stove designs at equal stove height with different BOG designs.

WBT conducted on G35A stove investigated BOG and pot support height as well as secondary air configuration. Additionally, WBT were performed on the reduced radiation shield gap found on both the G35B as well as the 3cm taller G35C. Figure 7 shows a plot of the high-power PM versus efficiency for all the different configurations tested.

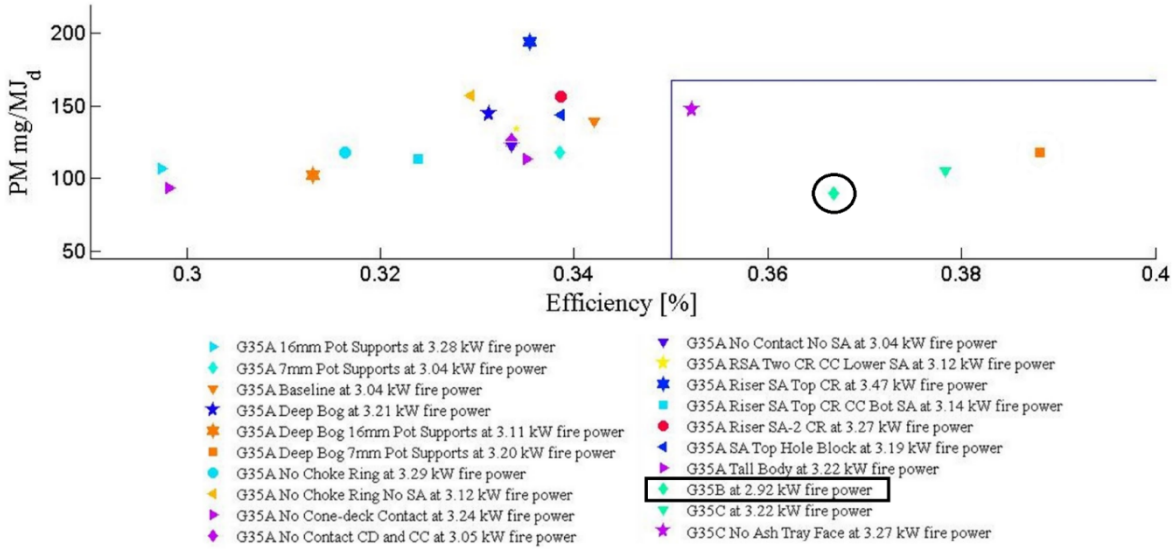

Figure 29. Efficiency versus high power PM metric for all stove configuration tested using WBT protocol. If BOG design is not listed on G35A shallow BOG was used, G35B was deep bog 7mm pot support height

Figure 29 shows the efficiency versus high power PM. The box on the lower right shows tier 3 performance. An important result is the effect of pot support height on thermal efficiency. This plot shows a 5% decrease in efficiency when pot support height is increased to 9 mm on the G35A shallow bog design. Modifying the secondary air configuration and choke ring placement has little to no effect on PM or efficiency. The G35B boxed in the legend with results circled in plot represents the stove configuration implemented in the Kenya field testing. Below is a plot of IWA WBT metrics for the G35B stove design with a deep bog at 7 mm pot support height. Figure 30 shows the G35B performance for several key metrics quantified as tiered results. Although these intermediate values of tiered values are not technically appropriate, we linearize the values between the nonlinear tiered values and plot them here for ease of interpretation. Figure 30 shows that the 35B achieves tier 3 or higher for metrics pertaining to the cold start phase of the WBT. The G35B design was chosen as the best design to use for field study. Devin Udesen, a masters student from the UW team, traveled to Nairobi and fabricated twelve 35B stoves in the Burn Manufacturing Stove factory. These stoves were used by Berkeley Air Monitoring in a field performance study in rural Kenya.

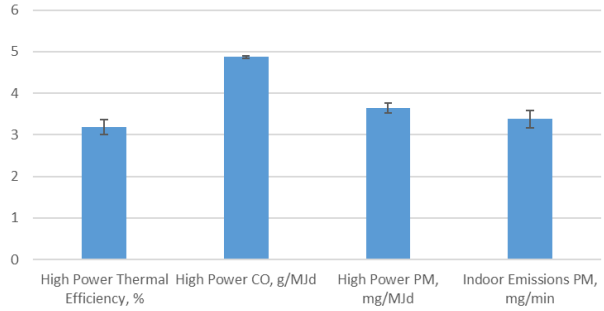

Figure 30. WBT tiered metrics for the G35B stove design as measured by a WBT.

Figure 31. Image of stoves G35B prototype stoves fabricated by Devin Udesen at the Burn Design Labs Nairobi factory. These stoves are being distributed to rural Kenyan households and will be measured for performance by Berkeley Air Monitoring

3.4 Field Performance Study

Our project partner Berkeley Air Monitoring Group was subcontracted to perform field testing in East Africa using the tier 3, 35B stove that was developed on this project. The field testing was conducted in the rural village of Gatanga in Kenya. This site was chosen due to its use of wood fuel and positive relationship with the local community organization. The study consisted of 15 participants of which 10 cooked with the 35B side feed rocket stove (SFR) and 5 cooked with traditional stoves such as three stone fires or other rudimentary stoves. Each participant was sampled twice, during two separate cooking events. Each SFR user was able to use the stove for a couple of weeks prior to the measurements to become more familiar with the operation of the stove. A variety of foods were cooked on the stoves in uncontrolled cooking tests (UCT) as listed in the table.

The UCTs are conducted with a sampling rake and a wind screen that is used to reduce the impacts of air currents. Partial capture measurement system and carbon balance-derived metrics are used. The UCT are conducted with foods selected by the participants. The stove emissions and fuel efficiency are measured and normalized to standard adult meals. The participants are instructed to cook as they normally would. The fuel is measured before and after the cooking event. The values recorded are CO, CO_2, and $PM_{2.5,}$ the fuel used per cooking event, as well as the number of standard adult meals prepared. In the UCT, the metrics are different than the WBT. In this case we report values per kg of fuel used or per standard adult meal.

The experimental results show that the 35B is the cleanest natural draft side fed rocket stove ever tested. The 35B reduced emissions more than 50% compared to the traditional stove. For every adult meal cooked, the 35B used 45% less fuel than the traditional stove. The metrics used in lab based WBT tests and field based UCT are not directly comparable; however, this field work shows that the 35B stove dramatically reduce PM emissions and cook food with significantly less fuel suggesting a dramatic increase in the thermal efficiency.

Table 3. Food used in the uncontrolled cooking field tests of the 35B stove.

Food	Traditional (N = 10)	SFR (N = 20)
Rice	50%	20%
Porridge	0%	15%
Fried eggs	10%	10%
Ugali	20%	10%
Vegetables	10%	5%
Drinks	10%	45%
Plantains	10%	10%
Stew	0%	5%
Arrowroot	10%	10%
Potatoes	10%	15%
Pancakes	0%	5%
Baby food	0%	5%
Boiling water	0%	10%

Figure 32. Images of the homes and traditional stoves used in the field evaluation work. (left) A three stone fire with a pot. The wind screen and sampling rake is shown behind and above the cooking pot. Smoke from the traditional fire is shown billowing out of the door. (right) A ceramic stove with a tin foil liner shown in the the home of the one of the participants.

Figure 33. The 35B improved cookstove in the participants home. Note the that in some cases a single large piece of wood is used and in other cases there are several smaller pieces of wood.

Table 4. Characteristics of fuel used in the UCT field work experiments.

	Traditional (N = 10)	**SFR (N = 20)**
Fuel Moisture Content	21% ± 8%	18% ± 3%
Wood Circumference (cm)	4 – 12 cm : 40% 13 – 30 cm: 60%	4 – 12 cm : 55% 13 – 30 cm: 45%
Wood Conditions	Irregular and varied in size and shape: 30% Mostly similar in size and shape: 70%	Irregular and varied in size and shape: 20% Mostly similar in size and shape: 80%
Starter fuel	Wood: 70% Crop Residue: 70% Kerosene: 20%	Wood: 75% Crop residue: 55% Kerosene: 35% Paper: 60%
Lighting technique	Lit from below: 60% Lit from above: 40%	Lit from below: 60% Lit from above: 35% Lit from middle: 5%

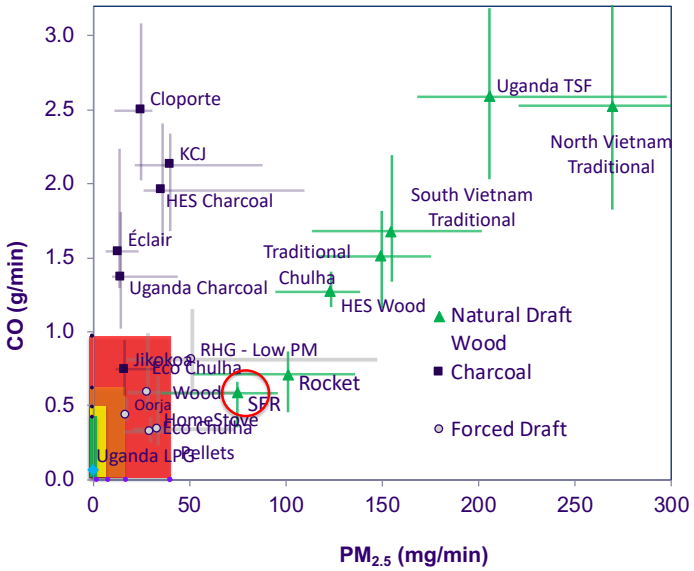

Figure 34. A phase map of the carbon monoxide and PM2.5 emissions rates generated in the UCTs. This figure is populated with data from previous Berekeley Air Monitoring campaigns for rocket, charcoal, and forced draft stoves. The 35B UCT experimental averages are worse than tier 4 lab based metrics; however, it is the cleanest natural draft rocket stove that Berkeley Air has ever tested.

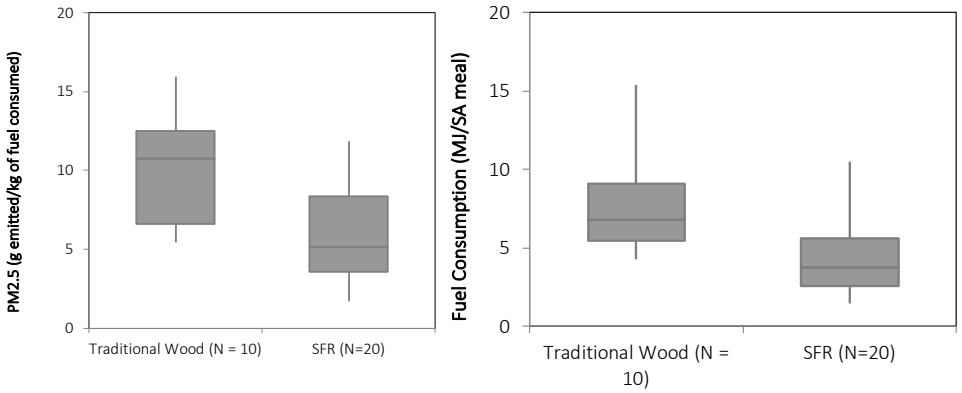

Figure 35. Field performance data for a traditional wood burning stove and the side fed rocket stove (SFR). (left) the PM2.5 emissions per kg of fuel consumed. (right) the fuel energy consumed per standard adult meal cooked. The PM2.5 is more than 50% lower for the SFR compared to the traditional stove and the fuel consumption is 45% lower.

3.5 Commercialization and Launch of the Kuniokoa

In the final stages of the project, we worked closely with Burn Design Labs and Burn Manufacturing company to translate the 35B design into a stone design that could be manufactured at scale with the durability and cost desired by users. The design for manufacturing process included tab and slot construction, modification of materials, and modification of some features that increased the cost or negatively impacted the durability of the stove. The choke ring was removed because there was concern that this component that was in direct contact with the flame may not hold up well over regular usage. The stove height was reduced 5 cm to reduce materials and increase efficiency. The shorter the

stove the lower the thermal mass and the closer the flames are to the pot and embers which results in better heat transfer and higher efficiency. This also has the impact of increasing PM production at higher fire powers because the flame will impact the pot and be quenched resulting in more soot production. The lower grate was removed for ease of assembly and the secondary air holes were moved and more serve to cool the combustion chamber than to introduce air into the flame. The production stove also has a radiation shield and no thermal insulation.

In Q4 of 2016 we transferred the wood stove product design to Burn Manufacturing. UW and BDL designed the stove as well as partnered with Burn Manufacturing Company (BMC) to design the necessary tooling (e.g. punches, casting, etc.) for manufacturing. Paul Means of Burn Design Labs lead this effort and travelled to Kenya several times in 2016 to transfer the knowledge to BMC in their Nairobi based factory. BMC named the stove the Kuniokoa which can be translated to "wood saver" in Swahilli.

We conducted a series of performance tests on the Kuniokoa. Performance testing included a UW's Firepower Sweep Test and 3 WBT tests. All WBT testing was in accordance with WBT Protocol 4.2.3. The goal of the performance testing was to determine the practical operating conditions that achieved Tier 3 in all performance metrics. After reviewing the results of the performance tests, it was found that Tier 3 was not achievable for all performance metrics for stove operation within the parameters that were determined by the FST and Rapid WBT's. Therefore, it is recommended that the Kuniokoa be reported as Tier 3 in all performance metrics except for Low-Power-Specific Consumption (Tier 2) and Indoor-Emissions-PM2.5 (Tier 2) for an operational firepower range of 3-3.5kW. It is also recommended that pot-to-flame interaction should be kept to a minimum when operating the stove within the recommended operational firepower range to keep PM2.5 emissions low.

Testing initiated with a fire power sweep to characterize the PM2.5 vs firepower vs flame-height performance trend. During this test the Kuniokoa was subjected to a range of operational firepower's from 0.5-4.5kW. Additionally, photographs of the flame exiting the top of the stove were taken continuously throughout the test to capture qualitative flame-height data that was correlated to instantaneous firepower and PM2.5 concentration. It was determined from the FST that the optimum operational firepower was between 3-3.5kW, which was determined by finding the upper-limit of firepower that produced better than Tier 3 PM2.5 performance. Firepower's below 3.5kW produce less PM2.5, even to within Tier 4, but these lower firepower's would result in unrealistic operating conditions and increased boil-time, both of which were undesirable for the user. Therefore, the lower-limit of 3kW was recommended. The flame-height photographs in comparison with firepower and PM2.5 data revealed that the amount of flame-impingement on the pot corresponded with an increase in PM2.5.

Three WBTs were performed by initiating the test with a cold-start HP-phase followed by a 45-minute simmer (low-power; LP) phase. The HP operational firepower was within the optimum range, at an average firepower of 3.21 +/- 0.03 kW, and the LP phase firepower depended on what was necessary to keep the water temperature within the simmer temperature range required by the WBT protocol (92-95 deg C). The results show that all performance metrics were above Tier 3 except for low-power-specific-consumption (Tier 2) and indoor-emissions-PM2.5 (Tier 2).

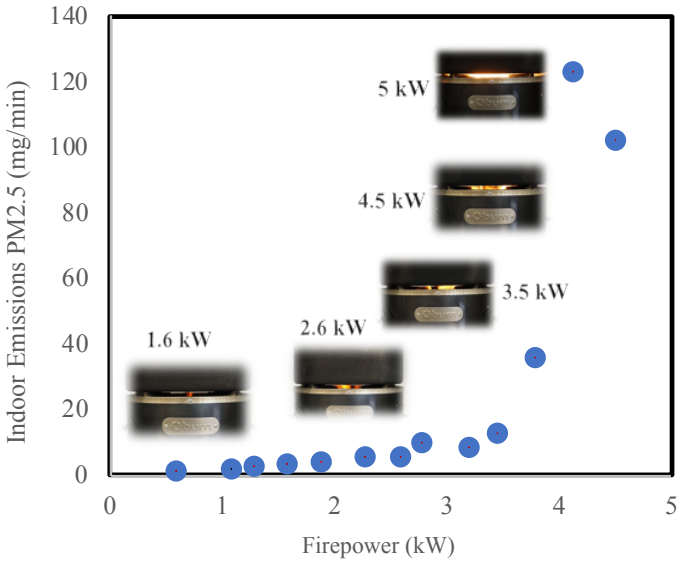

Figure 36. Fire power sweep. Indoor particulate emission rate as a function of fire power. The emissions remain low for firepowers below 3.5kW and then increase rapidly when the flame impinges on the pot.

Table 5. WBT Performance Metric Data

High Power Thermal Efficiency	**Test File**	**%**	**Avg.**	**Std. Dev.**	**Tier**	**Avg. Tier**	**Std. Dev.**
	3-28-17 WBT 1	38.86	40.44	1.13	3.39	**3.54**	0.11
	3-28-17 WBT 2	41.00			3.60		
	3-28-17 WBT 3	41.46			3.65		
Firepower	**Test File**	**kW**	**Avg.**	**Std. Dev.**	**Tier**	**Avg. Tier**	**Std. Dev.**
	3-28-17 WBT 1	3.25	3.21	0.03	N/A	**N/A**	N/A
	3-28-17 WBT 2	3.18			N/A		
	3-28-17 WBT 3	3.19			N/A		
Time to Boil	**Test File**	**min**	**Avg.**	**Std. Dev.**	**Tier**	**Avg. Tier**	**Std. Dev.**
	3-28-17 WBT 1	28.78	27.76	0.74	N/A	**N/A**	N/A
	3-28-17 WBT 2	27.08			N/A		
	3-28-17 WBT 3	27.42			N/A		
Low Power Specific Consumption	**Test File**	**MJ/min/L**	**Avg.**	**Std. Dev.**	**Tier**	**Avg. Tier**	**Std. Dev.**
	3-28-17 WBT 1	0.0272	0.0286	9.7e-04	3.07	**2.95**	0.09
	3-28-17 WBT 2	0.0292			2.90		
	3-28-17 WBT 3	0.0293			2.89		
High Power CO	**Test File**	**g/MJd**	**Avg.**	**Std. Dev.**	**Tier**	**Avg. Tier**	**Std. Dev.**
	3-28-17 WBT 1	1.81	1.85	0.11	4.77	**4.77**	0.01
	3-28-17 WBT 2	1.99			4.75		
	3-28-17 WBT 3	1.74			4.78		
Low Power CO	**Test File**	**g/min/L**	**Avg.**	**Std. Dev.**	**Tier**	**Avg. Tier**	**Std. Dev.**
	3-28-17 WBT 1	0.0323	0.0334	1.6e-03	4.64	**4.63**	0.02
	3-28-17 WBT 2	0.0323			4.64		
	3-28-17 WBT 3	0.0357			4.60		
High Power PM2.5 (TEOM)	**Test File**	**mg/MJd**	**Avg.**	**Std. Dev.**	**Tier**	**Avg. Tier**	**Std. Dev.**
	3-28-17 WBT 1	94.19	103.89	7.18	3.58	**3.50**	0.06
	3-28-17 WBT 2	111.34			3.45		
	3-28-17 WBT 3	106.15			3.49		
High Power PM2.5 (Gravimetric)	**Test File**	**mg/MJd**	**Avg.**	**Std. Dev.**	**Tier**	**Avg. Tier**	**Std. Dev.**
	3-28-17 WBT 1	143.06	124.51	32.36	3.20	**3.34**	0.25
	3-28-17 WBT 2	151.48			3.13		
	3-28-17 WBT 3	79.00			3.70		

Low Power PM2.5 (TEOM)	**Test File**	**mg/min/L**	**Avg.**	**Std. Dev.**	**Tier**	**Avg. Tier**	**Std. Dev.**
	3-28-17 WBT 1	1.30	1.42	0.11	3.70	**3.58**	0.11
	3-28-17 WBT 2	1.39			3.61		
	3-28-17 WBT 3	1.57			3.43		
Low Power PM2.5 (Gravimetric)	**Test File**	**mg/min/L**	**Avg.**	**Std. Dev.**	**Tier**	**Avg. Tier**	**Std. Dev.**
	3-28-17 WBT 1	1.53	1.14	0.27	3.47	**3.86**	0.27
	3-28-17 WBT 2	0.98			4.02		
	3-28-17 WBT 3	0.92			4.08		
Indoor Emissions CO	**Test File**	**g/min**	**Avg.**	**Std. Dev.**	**Tier**	**Avg. Tier**	**Std. Dev.**
	3-28-17 WBT 1	0.138	0.145	8.1e-03	4.67	**4.66**	0.02
	3-28-17 WBT 2	0.156			4.63		
	3-28-17 WBT 3	0.140			4.67		
Indoor Emissions PM2.5 (TEOM)	**Test File**	**g/min**	**Avg.**	**Std. Dev.**	**Tier**	**Avg. Tier**	**Std. Dev.**
	3-28-17 WBT 1	7.15	8.09	0.68	3.14	**3.01**	0.10
	3-28-17 WBT 2	8.72			2.92		
	3-28-17 WBT 3	8.41			2.95		
Indoor Emissions PM2.5 (Gravimetric)	**Test File**	**g/min**	**Avg.**	**Std. Dev.**	**Tier**	**Avg. Tier**	**Std. Dev.**
	3-28-17 WBT 1	10.85	9.66	2.44	2.68	**2.85**	0.32
	3-28-17 WBT 2	11.86			2.57		
	3-28-17 WBT 3	6.26			3.29		

Pilot Testing of the Kuniokoa

BMC received additional funding from Unilever and Acumen to purchase the tooling required for manufacturing the Kuniokoa. This support was made possible after their successful pilot study at several tea plantations. The pilot study was conducted in 146 homes in Mufindi, Tanzania, Limuru, Kenya, and Kericho, Kenya. This study enrolled 36% Unilever workers and 64% small holder farms. The goal of the pilot study was to understand the customers preferences for the stove and stove features, to learn about the effectiveness in fuel savings, and the customers willingness to pay for the stove.

The data showed that 88 percent of the users liked the stove and that 84% of the users were willing to pay for the stove. Nearly all the participants said that the stove reduced their fuel usage by 55% or more. The users preferred the Kuniokoa over other commercially available stoves and appreciated the stove features (ashtray, wood door, wood tray). 86% of the users perceived that the stove reduced emissions relative to their traditional stove. Comments included: less coughing and eye irritation, as well as cleaner environment, child friendly, no burns, or headaches.

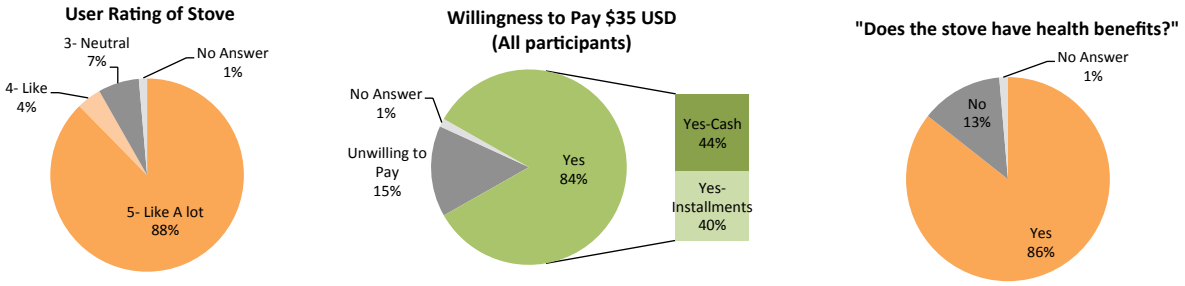

Figure 37. Pilot study responses to use of the Kuniokoa. The majority of users liked the stove, would be willing to pay for it and believed the stove had health benefits.

BMC started to manufacture the Kuniokoa in November of 2016 with a "soft" launch of the product. BMC held a launch event with over 100 attendees to celebrate the new stove and bring awareness to distributors and other stakeholders in Kenya. The manufacturing line has a current capacity of 150 stoves per day that can be increased to 350 per day. The high volume tooling was installed in 2017. BMC has sold over 12,000 stoves with a current month average sales of 750 units/month. They have orders in excess of 15,000 stoves next year and plan to sell more than 2,000 units/month. We have included images of the manufacturing line, the product stock and marketing images.



kuniokoa





kuniokoa
PIKA HARAKA, OKOA KUNI



kuniokoa

Examples of Kuniokoa product displays in Kenya.

Research Dissemination

During this project we have developed a cookstove design that is currently for sale by Burn Manufacturing Corporation as the Kuniokoa. We have disseminated our research at several conferences as well as prepared journal manuscripts. We continue to prepare several additional manuscripts for publication.

Journal Articles and Conference Papers

B. Sullivan, G. Allawatt, A. Emery, P. Means, J. Kramlich, and J.D. Posner. 2017 "Time-Resolved Particulate Emissions Monitoring of Cookstove Biomass Combustion Using a Tapered Element Oscillating Microbalance." *Combustion Science and Technology* 189, no. 6 (June 3, 2017): 923–36. doi:10.1080/00102202.2016.1253564.

A. Pundle, B. Sullivan, G. Allawatt, P. Means, A. Sullivan, J.D.Posner, J. Kramlich. The Role of Computational Fluid Dynamics in Cookstove Design. ETHOS, Kirkland WA, January 27, 2017

G. Allawatt, D. Udesen, A. Pundle, J. Kramlich, J.D. Posner. Closing the Gap Between Field and Lab Results for Rocket Coookstoves. ETHOS, Kirkland WA, January 27, 2017

J.D. Posner. Development, field evaluation, and commercialization of a natural draft, wood burning, rocket stove for rural East Africans. ETHOS, Kirkland WA, January 27, 2017.

C. Garland, M. Johnson. Investigating the performance of the University of Washington/BURN Stick-Fed Rocket (SFR) stove in Kenya during Uncontrolled Cooking Tests. ETHOS, Kirkland, WA, January 27, 2017.

A. Pundle, B. Sullivan, G. Allawatt, J. Kramlich, J.D. Posner. Predicting the Performance of a Natural Draft Cookstove for the Developing World using Computational Fluid Dynamics, 10th US National Combustion Meeting, College Park, MD, April 23-26, 2017.

G. Allawatt, D. Udensen, A. Pundle, B. Sullivan, P. Means, N. Figliola, J. Kramlich, J.D. Posner. A Transient State-Space Heat Transfer Model of Natural Draft Biomass Fueled Rocket Stoves, 10th US National Combustion Meeting, College Park, MD, April 23-26, 2017.

G. Allawatt, D. Udensen, A. Pundle, B. Sullivan, C. Garland, M. Johnson, P. Means, J. Kramlich, J.D. Posner. Reducing Pollutant Emissions in a Wood Burning, Natural Draft Cookstove Using Lab-Based Fire Power Sweep Measurements, 10th US National Combustion Meeting, College Park, MD, April 23-26, 2017.

B. Sullivan. Development of Cookstove Emissions and Performance Testing Suite with Time-resolved Particulate Matter Analysis and Excess Air Estimation. 2016. MS Thesis, University of Washington.

G. Allawatt, B. Sullivan, A. Pundle, J. Kramlich, J.D. Posner. 2016. A Transient State-Space Heat Transfer Model of a Natural Draft Wood Fueled Rocket Stove Used to Guide Stove Design, Western States Section Combustion Institute 2016 Spring Meeting, March 21,22, Seattle, WA.

A. Pundle, B. Sullivan, G. Allawatt, J.D. Posner, J. Kramlich. 2016. Two Dimensional Axisymmetric CFD Model of a Natural Draft Wood Fueled Rocket Cookstove, Western States Section Combustion Institute 2016 Spring Meeting, March 21,22, Seattle, WA.

B. Sullivan, G. Allawatt, J. Kramlich, J.D. Posner. 2016. Time-resolved particulate emissions monitoring of cookstove biomass combustion using a tapered element oscillating microbalance, Western States Section Combustion Institute 2016 Spring Meeting, March 21,22, Seattle, WA.

P. Means, P. Scott, G. Allawatt, B. Sullivan, A. Pundle, J. Kramlich, J.D. Posner. 2015. Development of an Innovative Natural Draft Cookstove for Woody Biomass Fuels. November 23, Clean Cooking Forum, Accra, Ghana, Africa.

B. Sullivan, G. Allawatt, A. Pundle, J. Kramlich, J.D. Posner 2015. Real- time Monitoring of Particulate Emissions from Wood-fired Cookstoves. ETHOS: Engineers in Technical and Humanitarian Opportunities of Service, January 24, Kirkland, WA.

A. Pundle, B. Sullivan, G. Allawatt, J.D. Posner, J. Kramlich 2015. Computational Fluid Dynamic Modeling of a Natural Draft Cookstove for Efficiency Optimization and Emissions Reduction. ETHOS: Engineers in Technical and Humanitarian Opportunities of Service, January 24, Kirkland, WA.

G. Allawatt, B. Sullivan, D. Udesen, A. Pundle, P. Means, J. Kramlich, J.D. Posner. 2016. A Simple Design Tool for Improving Cookstove Efficiency. ETHOS: Engineers in Technical and Humanitarian Opportunities of Service, January 30, Kirkland, WA.

A. Pundle, B. Sullivan, G. Allawatt, P. Means, J. Kramlich, J.D. Posner . 2016. Predicting Natural Draft Rocket Stove Performance Using Computational Fluid Dy- namics. ETHOS: Engineers in Technical and Humanitarian Opportunities of Service, Jan- uary 30, Kirkland, WA.

Journal Manuscripts in Preparation

G. Allawatt, D. Udensen, A. Pundle, B. Sullivan, P. Means, N. Figliola, J. Kramlich, J.D. Posner. A Transient State-Space Heat Transfer Model of Natural Draft Biomass Fueled Rocket Stoves.

A. Pundle, B. Sullivan, G. Allawatt, J. Kramlich, J.D. Posner. Two Dimensional Axisymmetric CFD Model of a Natural Draft Wood Fueled Rocket Cookstove

G. Allawatt, D. Udensen, A. Pundle, B. Sullivan, P. Means, J. Kramlich, J.D. Posner. Design and Development of a Tier 4 Natural Draft Wood Burning Cookstove for Low and Middle Income Countries

G. Allawatt, C. Garland, D. Udensen, A. Pundle, B. Sullivan, P. Means, J. Kramlich, M. Johnson, J.D. Posner. Development and Field Evaluation of an Improved Rocket Stove for East Africa

A. Pundle, J.D. Posner, J. Kramlich, Predicting Emissions from a Natural Draft Wood Fueled Rocket Cookstove using a Three-dimensional CFD Model.

4. Summary

The goal of the project was to develop a commercially viable, natural draft cookstove that exceeds ISO tier 4 criteria while meeting the needs of rural and urban cooks in East Africa. The cookstove should be market ready that meets the manufacturing cost and usability expectations of the final users, including durability, safety, comfort, aspirational value and compatibility with local fuels, foods, and customs. The cleaner burning cookstove product was designed to replace open fires and inefficient stoves so that it can enhance indoor air quality, personal

health, livelihoods, and the environment. The stove was developed using integrated and multidisciplinary design approach that included field based user research and focus groups, empirically verified computational fluid dynamics and heat transfer modeling, lab and field based emission and efficiency measurements, design for manufacturability, as well as in-home user product evaluations. This project provided training for eight University of Washington graduate students as well as six undergraduate students.

Nearly all project goals were met, although some of the project goals were changed from the original proposal. The CFD was initially proposed to be distributed using OpenFoam, an open source CFD platform. During the initial phases of CFD work we found that OpenFoam did not have sufficient algorithms and libraries to resolve the combustion chemistry required for this work. For this reason, we elected to use STAR-CCM+, a commercially available CFD software package. We did design, fabricate, build, and qualify a tier 4 stove; however, this stove did not met the users needs and aspirations. We used the lessons learned from this stove to build a tier 3 stove (in all but two metrics) that did meet the users needs and aspirations. This stove was shown to be the cleanest stove ever evaluated by Berkeley Air Monitoring Group. The design attributes from this stove were then used to design the Kuniokoa, a commercial stove that is now sold in East Africa by Burn Manufacturing company.

References:

[1] N. A. MacCarty and K. M. Bryden, "Modeling of household biomass cookstoves: A review," *Energy ForSustainable Dev.*, vol. 26, pp. 1–13, Jun. 2015.

[2] S. F. Baldwin, *Biomass stoves: engineering design, development, and dissemination*. Arlington, Va., USA : Princeton, N.J., USA: Volunteers in Technical Assistance ; Center for Energy and Environmental Studies, Princeton University, 1987.

[3] J. Agenbroad, M. DeFoort, A. Kirkpatrick, and C. Kreutzer, "A simplified model for understanding natural convection driven biomass cooking stoves—Part 1: Setup and baseline validation," *Energy Sustain. Dev.*, vol. 15, no. 2, pp. 160–168, Jun. 2011.

[4] J. Agenbroad, M. DeFoort, A. Kirkpatrick, and C. Kreutzer, "A simplified model for understanding natural convection driven biomass cooking stoves—Part 2: With cook piece operation and the dimensionless form," *Energy Sustain. Dev.*, vol. 15, no. 2, pp. 169–175, Jun. 2011.

[5] H. Burnham-Slipper, "Breeding a better stove: the use of computational fluid dynamics and genetic algorithms to optimise a wood burning stove for Eritrea," University of Nottingham, 2009.

[6] D. D. Miller-Lionberg, "A fine resolution CFD simulation approach for biomass cook stove development," Colorado State University, 2011.

[7] A. Wohlgemuth, S. Mazumder, and D. Andreatta, "Computational Heat Transfer Analysis of the Effect of Skirts on the Performance of Third-World Cookstoves," *J. Therm. Sci. Eng. Appl.*, vol. 1, no. 4, p. 041001, 2009.

[8] K. M. Bryden, D. A. Ashlock, D. S. McCorkle, and G. L. Urban, "Optimization of heat transfer utilizing graph based evolutionary algorithms," *Int. J. Heat Fluid Flow*, vol. 24, no. 2, pp. 267–277, Apr. 2003.

[9] A. Galgano and C. di Blasi, "Coupling a CFD code with a solid-phase combustion model," *Prog. Comput. Fluid Dyn.*, vol. 6, no. 4–5, pp. 287–302, 2006.

[10] T.-H. Shih, W. W. Liou, A. Shabbir, Z. Yang, and J. Zhu, "A new k-ϵ eddy viscosity model for high reynolds number turbulent flows," *Comput. Fluids*, vol. 24, no. 3, pp. 227–238, 1995.

[11] S. Pope, *Turbulent Flows*. New York: Cambridge University Press, 2001.

[12] I. Glassman and R. A. Yetter, *Combustion*, 4th ed. Academic Press, 2008.

[13] "STAR CCM+ User Manual," *CD-Adapco*. [Online]. Available: https://thesteveportal.plm.automation.siemens.com.

[14] M. Modest, *Radiative Heat Transfer*, Second. Academic Press, 2003.

[15] Y. Tominaga and T. Stathopoulos, "Turbulent Schmidt numbers for CFD analysis with various types of flowfield," *Atmos. Environ.*, vol. 41, no. 37, pp. 8091–8099, Dec. 2007.

[16] E. R. Hawkes, R. Sankaran, J. C. Sutherland, and J. H. Chen, "Scalar mixing in direct numerical simulations of temporally evolving plane jet flames with skeletal CO/H2 kinetics," *Proc. Combust. Inst.*, vol. 31, no. 1, pp. 1633–1640, Jan. 2007.

[17] J. Jetter *et al.*, "Pollutant Emissions and Energy Efficiency under Controlled Conditions for Household Biomass Cookstoves and Implications for Metrics Useful in Setting International Test Standards," *Environ. Sci. Technol.*, vol. 46, no. 19, pp. 10827–10834, Oct. 2012.

[18] F. P. Incropera and D. P. DeWitt, *Fundamentals and Heat and Mass Transfer*, Fifth. John Wiley and Sons, 2002.

[19] W. W. Yuen and C. L. Tien, "A simple calculation scheme for the luminous-flame emissivity," in *Symposium (International) on Combustion*, 1977, vol. 16, pp. 1481–1487.

[20] K. B. Sutar, S. Kohli, M. R. Ravi, and A. Ray, "Biomass cookstoves: A review of technical aspects," *Renew. Sustain. Energy Rev.*, vol. 41, pp. 1128–1166, Jan. 2015.

[21] V. H. Rapp, J. J. Caubel, D. L. Wilson, and A. J. Gadgil, "Reducing Ultrafine Particle Emissions Using Air Injection in Wood-Burning Cookstoves," *Environ. Sci. Technol.*, vol. 50, no. 15, pp. 8368–8374, Aug. 2016.

[22] D. Still, J. Kness, and Aprovecho Research Center., *Capturing heat : five earth-friendly cooking technologies and how to build them*. Cottage Grove, OR (80574 Hazelton Rd., Cottage Grove, OR 97424): Aprovecho Research Center, 1996.

[23] K. M. Bryden *et al.*, *Design Principles for Wood Burning Cookstoves*. Aprovecho Research Center.

[24] J. Jetter *et al.*, "Pollutant Emissions and Energy Efficiency under Controlled Conditions for Household Biomass Cookstoves and Implications for Metrics Useful in Setting International Test Standards," *Environ. Sci. Technol.*, vol. 46, no. 19, pp. 10827–10834, Oct. 2012.